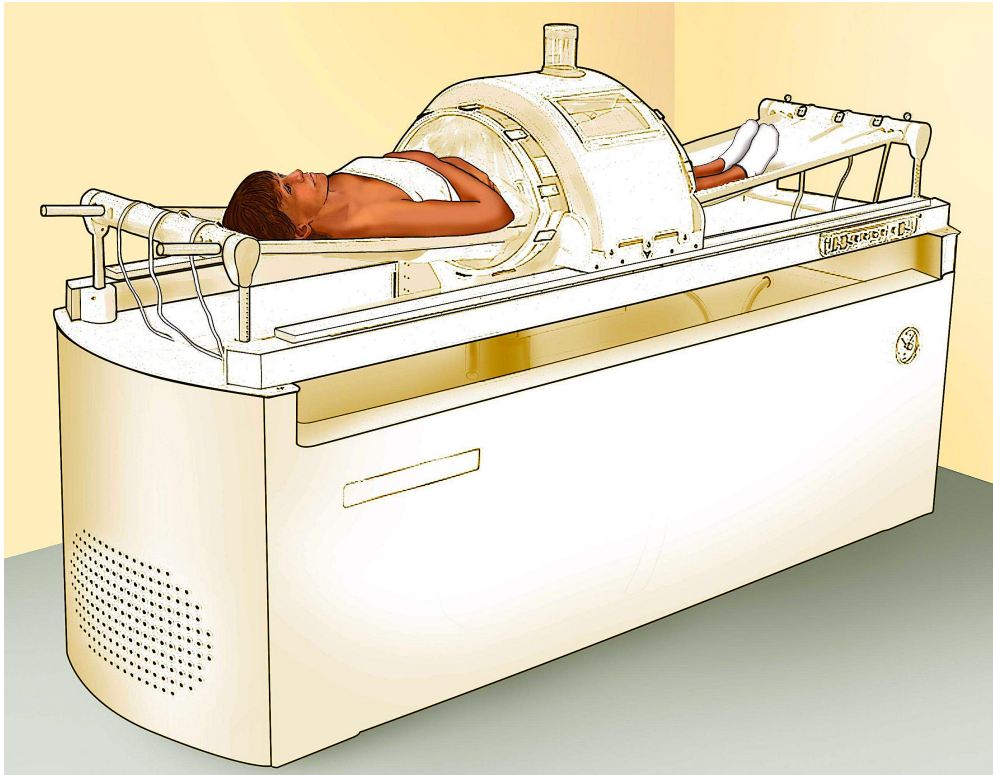




CHALMERS
UNIVERSITY OF TECHNOLOGY



Development of High Water Content Tissue Phantoms for Quality Assurance in Hyperthermia

Master's thesis in Biotechnology

Cengizhan Huseyin

Department of Electrical Engineering

CHALMERS UNIVERSITY OF TECHNOLOGY
Gothenburg, Sweden 2024
www.chalmers.se

MASTER'S THESIS 2024

Development of High Water Content Tissue Phantoms for Quality Assurance in Hyperthermia

Cengizhan Huseyin



CHALMERS
UNIVERSITY OF TECHNOLOGY

Department of Electrical Engineering
Division of Signal Processing and Biomedical Engineering
CHALMERS UNIVERSITY OF TECHNOLOGY
Gothenburg, Sweden 2024

Development of High Water Content Tissue Phantoms for Quality Assurance in
Hyperthermia
Cengizhan Huseyin

© Cengizhan Huseyin, 2024.

Supervisor: Mattia De Lazzari
Examiner: Hana Dobsicek Trefna, Department of Electrical Engineering

Master's Thesis 2024
Department of Electrical Engineering
Division of Signal Processing and Biomedical Engineering
Chalmers University of Technology
SE-412 96 Gothenburg
Telephone +46 31 772 1000

Cover: Illustration of a patient undergoing deep regional hyperthermia treatment

Typeset in L^AT_EX
Printed by Chalmers Reproservice
Gothenburg, Sweden 2024

Development of High Water Content Tissue Phantoms for Quality Assurance in Hyperthermia
Cengizhan Huseyin
Department of Electrical Engineering
Chalmers University of Technology

Abstract

As cancer persists as a notable health challenge worldwide, novel therapeutic approaches are required to complement current treatment modalities. Hyperthermia therapy is recognized to be an effective approach, which can be combined with either chemotherapy or radiation therapy in order to effectively treat tumors using electromagnetic radiation to generate heat. Depending on the size, depth and location of the tumor, various heating devices are used for treatment. Radiative microwave and radio-wave systems are commonly used for the treatment of deep-seated tumors in larger anatomical regions, operating within the lower frequency range of 70-120 MHz. To ensure that these devices can deliver adequate heat within the targeted area, adherence to quality assurance guidelines protocols are important. These guidelines are pivotal for maintaining the quality of heating devices as well as protecting the health of individuals receiving treatment. The evaluation of device performance is conducted through the utilization of physical materials known as phantoms. The purpose of using phantoms is to replicate the biological and dielectric properties of tissues in the human body. Depending on the specific tumor being treated, various phantom materials can be used and combined with each other in order to simulate the properties of the tissues where the tumor is located. It is essential for these phantoms to possess sufficient mechanical strength to be able to endure the experimental conditions, as they will be subjected to heat in clinical trials.

In this thesis, hydroxyethylcellulose was used as a ground component in conjunction with agar, glycerol and salt to fabricate a mechanically stable phantom that mimics the dielectric properties of muscle tissue, with the aim of treating deep-seated tumors. To achieve a functioning phantom possessing the desired properties, an optimization of the process was performed by analyzing various parameters in regards to concentration, molecular weight and air bubble formation.

Keywords: Hyperthermia Therapy, Chemotherapy, Radiation Therapy, Radiative Systems, Phantoms, Hydroxyethylcellulose, Agar, Glycerol, Salt.

Acknowledgements

I would like to express my sincere gratitude to my examiner, Hana Dobsicek Trefna, for accepting me into this master thesis. It has been a great learning experience and very interesting to gain insight into the field of biomedical engineering as well. Thank you for your support and guidance, I wish you all the best.

A special thanks to Mattia De Lazzari for his invaluable assistance with measurements and for patiently answering all the questions I had. Your willingness to help was important for the completion of the thesis. I appreciate it.

I would also like to thank all the other people who have helped and supported me along the way. Your contributions and willingness to share your knowledge have been greatly appreciated.

Cengizhan Huseyin, Gothenburg, October, 2024

List of Acronyms

Below is the list of acronyms that have been used throughout this thesis listed in alphabetical order:

EM	Electromagnetic
HEC	Hydroxyethylcellulose
HT	Hyperthermia Therapy
MC	Methylcellulose
MW	Microwave
Mw	Molecular Weight
PEG	Polyethylene Glycol
QA	Quality Assurance
RF	Radio-Frequency
SAR	Specific Absorption Rate

Nomenclature

Below is the nomenclature of symbols and variables that have been used throughout this thesis.

Symbols & Variables

ε	Permittivity
ε_r	Relative Permittivity or Dielectric Constant
ε'_r	Real Part of Relative Permittivity
ε''_r	Imaginary Part of Relative Permittivity (Loss Factor)
ε_0	Permittivity of Vacuum or Free Space
σ_r	Conductivity
ω	Angular Frequency



Contents

List of Acronyms	ix
Nomenclature	xi
List of Figures	xv
List of Tables	xvii
1 Introduction	1
1.1 Background	3
1.1.1 Quality Assurance and Deficiencies of Hyperthermia-Based Systems	4
1.1.2 QA and Phantoms	4
1.1.3 Project Aim	5
1.1.4 Scope	5
2 Theory/Literature Review	7
2.1 Dielectric Properties	7
2.1.1 Electrical Properties of Biological Tissues	9
2.1.2 Electrical Properties of Biological Tissues at Different Frequencies	10
2.2 Specific Absorption Rate	12
2.3 Hyperthermia Treatment	14
2.3.1 Deep Regional Hyperthermia	14
2.3.2 Superficial Local Hyperthermia	15
2.4 Phantom Materials	16
2.4.1 Liquid Phantoms	16
2.4.2 Semi-solid Phantoms	17
2.4.3 Solid Phantoms	18
2.5 Hydrogels in Hyperthermia Therapy	19
2.5.1 Hydroxyethylcellulose	19
2.5.2 Correlation between Molecular Weight, Viscosity and Concentration of HEC	21
2.5.3 Methylcellulose	22
2.5.4 Perfax (Methylcellulose-Based)	22
2.5.5 Materials to Increase Mechanical Stability	23
2.5.6 Materials to Reduce Permittivity	23

2.5.7	Salt to Increase Conductivity	25
2.5.8	Occurrence of Air Bubbles in Phantoms	25
3	Materials and Methods	27
3.1	Phantom Development Process	27
3.2	Material Selection	27
3.3	Phantom Development	30
3.3.1	Perfax Phantom	30
3.3.2	Hydroxyethylcellulose Gel	31
3.3.3	Muscle Phantom	33
3.3.3.1	Compositions of Muscle Phantom For The Optimized Recipes	34
3.4	Dielectric Properties Assessment	35
4	Results & Discussion	37
4.1	Dielectric Properties of Perfax Phantom at Elevated Temperatures . .	37
4.2	Phantom Process Optimization	39
4.2.1	Analysis of HEC Gel Solidity	39
4.2.2	Analysis of HEC Gel Concentration	40
4.2.3	Air Bubbles Formation Assessment	41
4.2.4	HEC Gel Confirmation	42
4.3	Dielectric Properties Assessment	43
4.3.1	Dielectric Properties (Mean & Deviation) of HEC Gels	43
4.3.2	Dielectric Properties of Muscle Phantoms	45
5	Conclusion/Future Outlook	47
	Bibliography	49
A	Appendix 1	I
A.1	Dielectric Properties of HEC Gels	I

List of Figures

1.1	a) Incidences of the most prevalent forms of cancer worldwide in 2022. b) Mortality rates for the occurring cancer types globally in 2022.	2
2.1	Anatomy of Human Skin	10
2.2	Frequency Dependence of Permittivity and Conductivity of a Heterogeneous Material (Biological Tissues)	10
2.3	SAR and Temperature distributions of a phantom model exposed to mobile phone radiation at 900 MHz frequency. The red color indicates the area distribution in which most of the RF energy is absorbed, and the blue color the least energy absorbed	13
2.4	Two RF hyperthermia systems. Radiative-based BSD-2000 3D/MR (left) and Capacitive-based Thermotron RF-8EX (right)	14
2.5	Superficial Hyperthermia Treatment	15
2.6	Structure of Hydroxyethylcellulose (HEC)	20
2.7	Structure of Methylcellulose (MC)	22
2.8	Measured Permittivity of Various Water/Glycerol Mixtures in relation to Frequency	24
3.1	Experimental Setup and Procedure of Muscle Phantom	29
3.2	Schematic of the Measurement Setup for the Dielectric Properties (DAK-TL2)	35
4.1	a) Permittivity at Elevated Temperatures b) Conductivity at Elevated Temperatures	38
4.2	HEC Gels, Each Containing Distinct Molecular Weights	39
4.3	Phantom Appearance of Natrosol 250 HHX at Various Concentrations: Left: 3wt% to Right: 4wt%	40
4.4	Phantom Appearance of Natrosol 250 HHX at Various Mixing Velocities: Left: Phantom 1 to Right: Phantom 3	41
4.5	Gel Appearance of Natrosol 250 HHX: Left: Gel 1 to Right: Gel 3	42
4.6	a) Average Permittivity along with Standard Deviation Over the Frequency Range (200-490 MHz) b) Average Conductivity along with Standard Deviation Over the Frequency Range (200-490 MHz)	44
4.7	Final Muscle Phantom (Produced from Phantom Recipe 4)	45
4.8	a) Permittivity of the Optimized Phantom Recipes Over the Frequency Range (60-550 MHz) b) Conductivity of Two 35Gly Phantoms Over the Frequency Range (60-550 MHz)	46

List of Figures

A.1	Permittivity of HEC Gels Over the Frequency Range (200-490 MHz)	I
A.2	Conductivity of HEC Gels Over the Frequency Range (200-490 MHz)	II

List of Tables

2.1	Permittivity of Various Tissues at 100 & 915 MHz	11
2.2	Conductivity of Various Tissues at 100 & 915 MHz	11
2.3	Correlation between Molecular Weight, Viscosity and Concentration of HEC	21
3.1	Ingredients of Perfax Phantom	30
3.2	Ingredients of Hydroxyethylcellulose Phantom at 2 wt%	31
3.3	Compositions For the Optimized Phantoms	34
4.1	Viscosity of HEC Products, Differing in Mw	39
4.2	Air Bubbles and Solidity assessment of HEC at Various Concentrations	40
4.3	Quantity and Size of Air Bubbles at Different Mixing Rates	41
4.4	Composition of Muscle Phantom Illustrated in Graph 4.8 b)	45

1

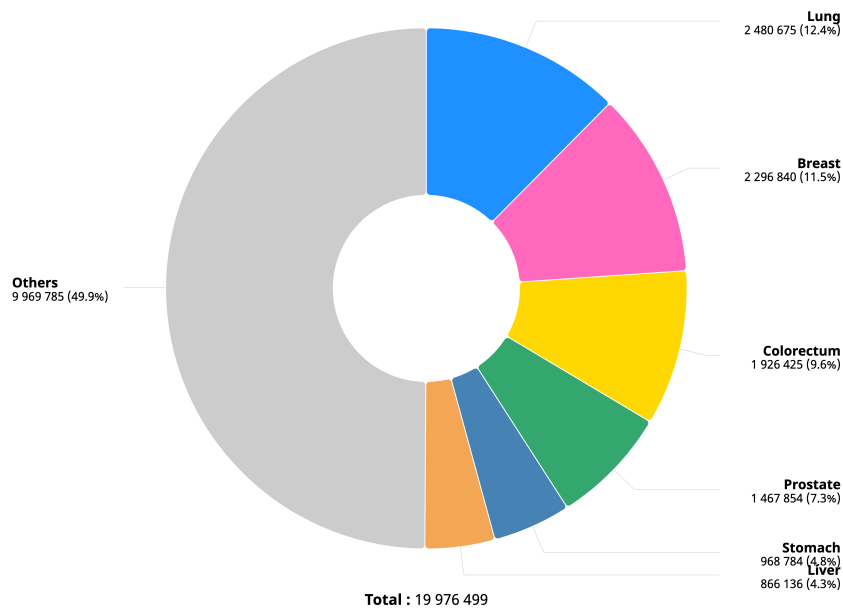
Introduction

Although there have been advancements in cancer therapy, it remains as one of the leading causes of death worldwide. Cancer encompasses a broad range of disorders that may originate in any organ or tissue, characterized by the uncontrolled growth of abnormal cells, which can subsequently spread into other nearby regions of the body. This event is often known as metastasis [1]. Human cells usually undergo cell division, a process in which they grow and replicate, leading to the creation of new cells to fulfill the body's needs. When cells approach the end of their lifetime or suffer harm, they undergo cellular apoptosis, and are subsequently regenerated by new cells. Occasionally, this orderly mechanism malfunctions, leading to the proliferation of abnormal or injured cells beyond what is expected. These cells have the potential to develop into cancers [2]. A tumor is a cohesive aggregation of aberrant cells that results in the formation of a solid mass of tissue. Tumors may be classified into many categories based on their nature: cancerous (malignant), noncancerous (benign), or precancerous. Precancerous tumors are initially benign but have the potential to develop into cancerous tumors if not appropriately managed. Benign tumors are not malignant and they generally do not have an impact on adjacent tissue or metastasize to other areas of the body. Malignant tumors, also known as cancerous tumors, have the ability to invade and spread to adjacent tissues, glands, and other bodily structures [3].

The estimated number of new cases and mortality rates for the most prevalent cancer categories in 2022 are depicted in Figure 1. Breast, lung, and colorectal cancer are the most prevalent types, and colorectal and lung malignancies are the main causes of mortality [4]. In contrast, detection method advancements and more effective treatment modalities have contributed to a steady decline in mortality rates for the majority of common cancer types, including colorectal, lung, and breast cancer, over the past four decades [5].

1. Introduction

Absolute numbers, Incidence, Both sexes, in 2022
Continents

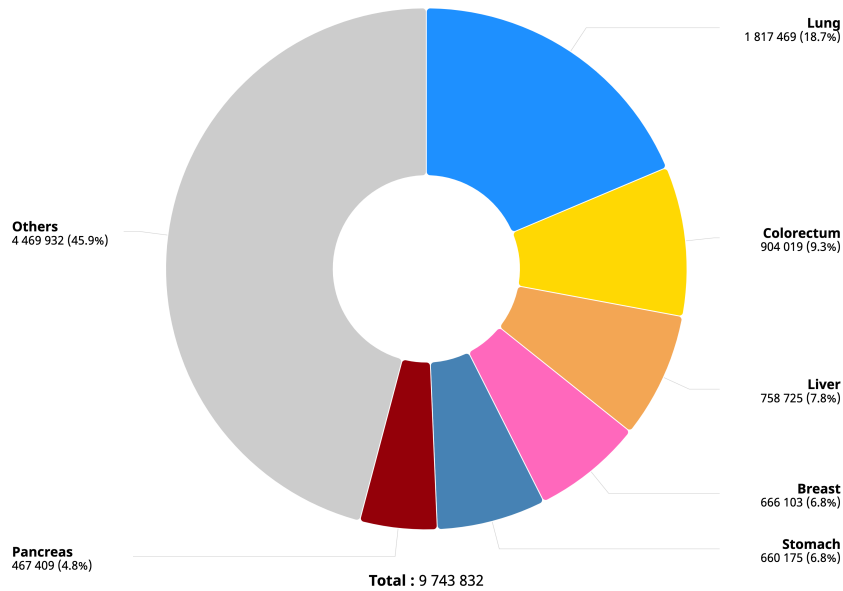


Cancer TODAY | IARC - <https://gco.iarc.who.int/today>
Data version : Globocan 2022 (version 1.1)
© All Rights Reserved 2024



(a)

Absolute numbers, Mortality, Both sexes, in 2022
Continents



Cancer TODAY | IARC - <https://gco.iarc.who.int/today>
Data version : Globocan 2022 (version 1.1)
© All Rights Reserved 2024



(b)

Figure 1.1: a) Incidences of the most prevalent forms of cancer worldwide in 2022.
b) Mortality rates for the occurring cancer types globally in 2022.
Data obtained from: [1].

1.1 Background

Currently, there are several modalities for cancer therapy. The most common therapies utilized are chemotherapy, radiation therapy and surgery [6]. Surgery is frequently the initial course of action in the treatment of cancer, but depending on cancer type and the size of the cancer, it is not uncommon to supplement it with additional therapies [7]. Chemotherapy eliminates cancer cells through the use of drugs that inhibit or delay the cells growth. Generally, chemotherapy is administered for two purposes. One rationale is to mitigate the likelihood of cancer recurrence through treatment. The alternative purpose is to diminish the size of lesions that are causing discomfort and other complications [8]. High doses of radiation are employed in radiation therapy for the purpose of eradicating cancer cells and shrinking tumor sizes. Radiation therapy destroys cancer cells by causing DNA damage at high dosages. When DNA is damaged beyond repair, cancer cells cease dividing or perish. Upon cell death, they undergo degradation and elimination by the organism [9].

These conventional cancer treatments however, have a number of limitations and challenges, due to their expensive nature, adverse reactions and potential risk of cancer recurrence. Hyperthermia therapy (HT) is becoming recognized as a potential complement treatment for cancer that can address the limitations of traditional cancer treatments when combined with them. Hyperthermia therapy can be combined with chemotherapy or radiation therapy to increase the effectiveness and efficacy of cancer treatments [10]. Hyperthermia involves increasing the body or tumor tissue temperature to specifically treat malignant tumors using heat, with the aim of reaching 40-45°C for a duration of one hour. The therapy is typically categorized into three main types based on how it is conducted, including local, regional and whole-body hyperthermia [11].

A variety of electromagnetic (EM) technologies have been utilized for the purpose of administering hyperthermia. The main distinction is the frequency of the applicator utilized [12]. Radio-wave frequency (RF) covers a range of 3kHz to 300 GHz and is typically used for superficial heating [13], while microwave (MW) frequency covers a range of 300 MHz to 300 GHz and is normally used for deep tissue heating, and is a part of the RF range [14]. One important aspect of analyzing how electromagnetic waves interact with biological tissues involves utilizing "phantoms" that mimic the properties of these tissues. A phantom is typically described as a physical material constructed from various materials that in tandem replicate the biological and dielectric characteristics of specific biological tissues. Common tissues that are replicated using phantoms include muscle and fat tissues due to their distinct difference in water content. Tissue mimicking phantoms offer a simulation tool for quality assurance (QA) and improving therapy, eliminating the need of subjecting a living organism to risk [15].

1.1.1 Quality Assurance and Deficiencies of Hyperthermia-Based Systems

Elevated tumor temperatures has seemingly been linked to better clinical outcomes. The efficacy of hyperthermia treatments in combination with chemo and radiation therapy however, is still limited by a number of factors, regardless of the type of tumor being treated. In order to effectively make a tumor more responsive to chemo and radiation, it is important to administer a sufficient amount of heat to the entire tumor while also limiting the temperature rise in healthy tissues nearby [16]. Some HT devices fail to deliver the sufficient amount of heat/thermal dose required to achieve the intended clinical outcome [17]. The deficiencies in HT devices can be hindered and controlled by implementing adequate quality assurance guidelines.

According to the International Standard Organization (ISO), quality assurance is defined as the term used to describe the process of ensuring that a product meets specific requirements and standards. It typically answers the question "Are we correctly following the process and taking measures to prevent inadequacies?" [18]. In the context of hyperthermia treatment the "inadequacies" refer to identifying flaws of heating devices and implementing a corrective approach. Phantoms play an important role in quality assurance and regulatory compliance of medical devices. They offer a way to assess and confirm the accuracy as well as reliability of heating systems. By implementing quality assurance guidelines, deficiencies of heating devices can be averted [19].

1.1.2 QA and Phantoms

To be able to successfully implement guidelines and analyze the effectiveness of heating systems, ensuring safety and long-term stability, appropriate phantom materials need to be utilized. The phantom materials have to fulfill certain requirements when HT is delivered through EM radiation, in regards to its properties and qualities [71].

1. Be able to accurately simulate the dielectric properties of the tissues where the tumor is located.
2. Sufficient mechanical strength to be able to endure high temperatures when the phantom is subjected to heat. Must be able to maintain its primary structure without degrading.
3. The dielectric and mechanical properties should be able to maintain stable over time.
4. The phantom materials should be biocompatible, non-toxic with the use of cost-effective and affordable ingredients.

1.1.3 Project Aim

The objective of this thesis is to develop a mechanically stable, homogeneous muscle phantom that closely mimics the dielectric properties of human muscle tissue. This includes investigating and testing appropriate phantom materials and combining them to create a functional phantom suitable for quality assurance assessments. The goal of formulating a simple, cost-effective recipe that can be easily replicated using affordable materials arises from the need for reliable quality assurance protocols. In this sense, the developed muscle phantom can serve as a tool for verification of devices for deep microwave hyperthermia treatment.

1.1.4 Scope

1. Finding appropriate phantom materials to develop a mechanically stable muscle phantom that should be able to assess the performance of devices for quality assurance.
2. The phantom materials utilized should be able to roughly mimic the dielectric properties of muscle tissue as well as produce a stable and durable phantom gel.
3. Finding the optimal concentration and solidity of the muscle phantom based on the materials used, that should contain as few air bubbles as possible.
4. Visually evaluate the mechanical stability/durability of the muscle phantom.

2

Theory/Literature Review

This chapter seeks to provide the necessary foundation for understanding the relationship of parameters discussed in the thesis, in regards to QA in HT therapy. Additionally, various phantom materials and properties are introduced and explained. The sections, dielectric properties (permittivity & conductivity) in tissues is explained followed by SAR and its relation to MW heating. Two forms of hyperthermia therapies, (superficial local & deep regional) is then explained, followed by a section about different phantom types and finally the importance of hydrogels and materials utilized to develop the desired muscle phantom.

2.1 Dielectric Properties

The dielectric properties of biological tissues are critical for understanding how they interact with electromagnetic fields. These properties are characterized by permittivity and conductivity, which define how a material polarizes and conducts electricity when subjected to an electric field. The majority of the electrons in the tissue are bonded to the nucleus [20]. An atom's bound electrons are moved when an external electric field is applied causing the centroid of the electronic cloud to diverge from the centroid of the nucleus. As a result the atom is polarized and an electric dipole is generated. This phenomenon is typically known as polarization [20].

Permittivity (ϵ) refers to a material's ability to store electrical energy in an electric field. It determines the relationship between the electric displacement field and the electric field, which can be expressed by the equation: [21].

$$\mathbf{D} = \epsilon \mathbf{E}$$

where,

D is the electric displacement field,

ϵ is the permittivity of the material,

E is the electric field strength

The relative permittivity ϵ_r , also known as the dielectric constant is the ratio of a material's permittivity to that of a vacuum. It indicates how much more or less efficiently a material can store electrical energy compared to a vacuum, and is typically defined by the following equation [72]:

$$\epsilon_r = \frac{\epsilon}{\epsilon_0} \quad (2.1)$$

where, ϵ_0 is the permittivity of vacuum or free space

The relative permittivity is made up of a real part, indicating the material's ability to store energy and an imaginary part, representing the loss factor or how much energy is lost as heat. The real and imaginary part in relation to the relative permittivity can be defined by the equation: [21].

$$\epsilon_r = \epsilon'_r - j\epsilon''_r \quad (2.2)$$

where,

ϵ'_r is the real part of relative permittivity

ϵ''_r is the imaginary part of relative permittivity

The imaginary part of relative permittivity is connected to the conductivity, σ_r . Conductivity refers to a material's ability to conduct electric current. When an alternating current electric field is generated, a material's conductivity dictates how easily electric charges can pass through it. Highly conductive materials enable electrons to move freely within their molecular structure opposed to low conductive materials, that have minimal amounts of free electrons. The electrons are thus securely bound, and it will require a sufficient amount of energy to extract them [21]. The relationship between conductivity and permittivity at a particular angular frequency, ω is generally defined by:

$$\sigma_r = \omega\epsilon_0\epsilon''_r \quad (2.3)$$

where,

$$\omega = 2\pi f \quad (2.4)$$

and f is the frequency of the generated electric field.[20].

In biological tissues, both permittivity and conductivity change with frequency. The real part of permittivity, ϵ'_r increases at lower frequencies as a result of the tissue's dipoles having more time to align with the electric field [22]. Lower energy storage capacity results from the dipoles inability to align as rapidly as the frequency increases and ϵ'_r decreases. The conductivity, σ_r on the other hand, increases with frequency due to the higher energy input causing more charge carriers to relocate [22].

2.1.1 Electrical Properties of Biological Tissues

As the human body and skin is very complex as seen in figure 2.1, biological materials exhibits significant variations in their electrical properties [23][25]. The variations are mainly influenced by the fluidity of the material in regards to permittivity. Tissues such as muscle tissue tend to have higher permittivity due to the higher water content. In regards to conductivity, blood and brain have a relatively good conductivity for electric current opposed to tissues such as fat and bone, that do not conduct heat as efficiently [23].

Another factor that can be contributed to the variations of electrical properties in tissues are their structural organization. The properties are influenced by both the arrangement of cells and the extracellular matrix [24]. The arrangement of cells can affect how electric fields can propagate through tissue, and the chemical composition of the extracellular matrix can also influence how tissues store and conduct electrical energy. For instance, the permittivity and conductivity vary in bone tissue in comparison to muscle tissue due to its dense and ordered structure, whereas muscle tissue have a more loosely organized structure [24].

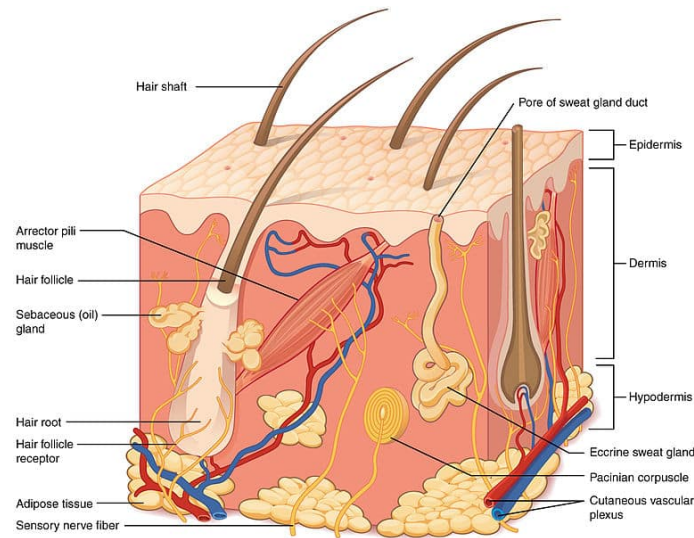


Figure 2.1: Anatomy of Human Skin

Data obtained from: [25].

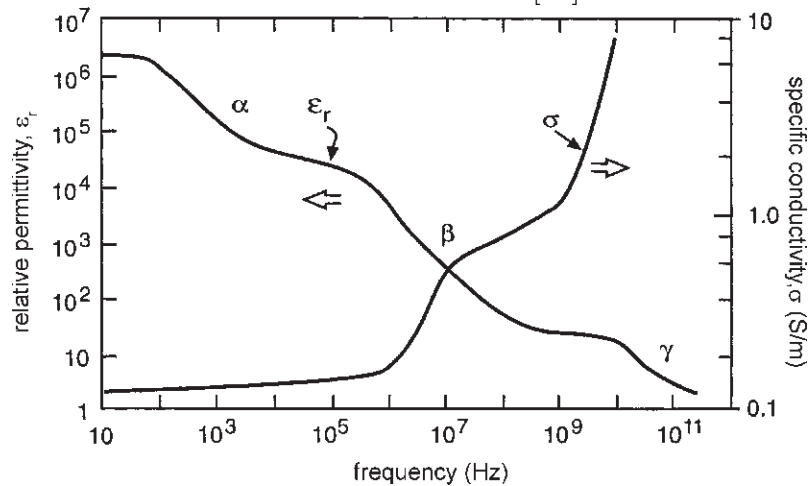


Figure 2.2: Frequency Dependence of Permittivity and Conductivity of a Heterogeneous Material (Biological Tissues)

Data obtained from: [26].

2.1.2 Electrical Properties of Biological Tissues at Different Frequencies

In the context of phantom development, the outcome of dielectric properties is influenced by a number of factors, including the chemical composition of the phantom and the development procedure. In figure 2.2, it can be seen that the permittivity of biological tissues decreases rapidly at higher frequencies while the conductivity increases. At lower frequencies, materials are able to align their dipoles in response to the electric field for a longer period of time, resulting in an increased dielectric constant. At higher frequencies however, there is a reduced opportunity for the dipoles to react completely, resulting in decreased polarizability of the material [27].

Tissue	Permittivity, ϵ_r 100 MHz	Permittivity, ϵ_r 915 MHz
Blood	76.8	61.3
Brain (Cerebellum)	89.8	49.3
Fat	12.7	11.3
Heart	90.8	59.8
Kidney	98.1	58.6
Liver	69.0	46.8
Muscle	66.0	55.0
Stomach	77.9	65.0

Table 2.1: Permittivity of Various Tissues at 100 & 915 MHz
Data obtained from: [28].

Tissue	Conductivity, σ_r 100 MHz	Conductivity, σ_r 915 MHz
Blood	1.23	1.54
Brain (Cerebellum)	0.79	1.27
Fat	0.07	0.11
Heart	0.73	1.24
Kidney	0.81	1.40
Liver	0.49	0.86
Muscle	0.71	0.95
Stomach	0.90	1.19

Table 2.2: Conductivity of Various Tissues at 100 & 915 MHz
Data obtained from: [28].

2.2 Specific Absorption Rate

Specific Absorption Rate (SAR) is an important parameter in the context of microwave hyperthermia treatment and electromagnetic field exposure. SAR is generally monitored to ensure that exposure levels are within acceptable limits, especially for therapies and devices that involve prolonged exposure to microwave radiation [29][30].

To predict the SAR, which directly correlates microwave radiation with increasing heat in the target area, Penne's bioheat equation is commonly used: [73].

$$\rho c_p \frac{\partial T}{\partial t} = \nabla \cdot (k \nabla T) + W_b c_b (T_b - T) + C + \rho \text{SAR} \quad (2.5)$$

where,

ρ is the mass density of the tissue (kg/m^3)

c_p is the specific heat capacity of the tissue ($\text{J}/(\text{kg} \cdot ^\circ\text{C})$)

T is the temperature of the tissue ($^\circ\text{C}$)

t is time (s)

k is the thermal conductivity of the tissue ($\text{W}/(\text{m} \cdot ^\circ\text{C})$)

W_b is the blood perfusion constant ($\text{kg}/\text{m}^3/\text{s}$)

c_b is the specific heat capacity of blood ($\text{J}/(\text{kg} \cdot ^\circ\text{C})$)

T_b is the temperature of the blood ($^\circ\text{C}$)

C is the metabolic heat generation (W/m^3)

SAR is the Specific Absorption Rate (W/kg), which represents the power absorbed per unit mass of tissue due to electromagnetic fields

Here, it is worth to mention that the only external source causing the heat is the SAR. Additionally, SAR is proportionate to the electric field strength in the target area [74]:

$$\text{SAR} = \frac{1}{V} \int_{\text{sample}} \frac{\sigma(\mathbf{r}) |\mathbf{E}(\mathbf{r})|^2}{\rho(\mathbf{r})} d\mathbf{r}, \quad (2.6)$$

where,

V is the volume of the sample under consideration (m^3)

$\sigma(r)$ is the electrical conductivity of the tissue at position r (S/m)

$\rho(r)$ is the mass density of the tissue at position r (kg/m^3)

r represents the spatial coordinates within the sample

These equations are often used in conjunction to determine the electric fields and exposure time required for effective therapy [73][74]. A key feature of the equations is the electric properties of the tissues, particularly the conductivity, which directly links the electric field strength to SAR. As the conductivity increases, a greater SAR is achieved, due to the tissue absorbing more electromagnetic radiation. This implies that, under the same conditions, tissues with higher conductivity (e.g. muscle tissue) will have higher SAR values opposed to tissues with lower conductivity, such as fat tissue [29][31]. During therapy, the tissue properties are constant and depends on the

patient, therefore only the electric field strength has to be determined. For realistic experiments, both tissue properties and electric fields needs to be determined during measurements, where the phantoms is required to simulate real tissue properties [30][73].

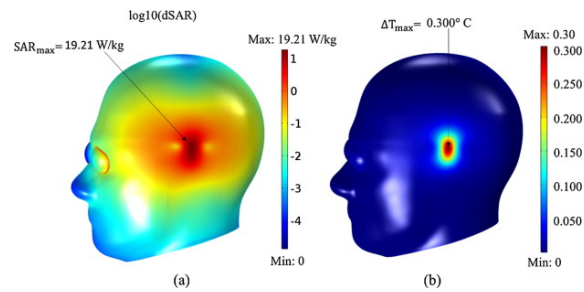


Figure 2.3: SAR and Temperature distributions of a phantom model exposed to mobile phone radiation at 900 MHz frequency. The red color indicates the area distribution in which most of the RF energy is absorbed, and the blue color the least energy absorbed

Data obtained from: [32].

2.3 Hyperthermia Treatment

Effective hyperthermia treatment can often be achieved depending on the location, depth and size of the tumor.

2.3.1 Deep Regional Hyperthermia

Deep regional HT aims to treat tumors that are located beyond approximately 4 cm beneath the skin surface and specifically targets a regional area of the body such as the pelvic region [33]. The most commonly used techniques are radiative RF and MW devices. Beyond 2 cm from the skin, successful clinical outcomes is often associated with radiative heating of deep-seated tumors in the pelvic region, such as those in prostate, bladder, rectum and cervix tumors. Radiative external antennas that emit radiation creates an electromagnetic field that is transferred to the patient through the use of a water-filled bolus. Target heating can be effectively achieved by adjusting the phase and amplitude of the antennas to ensure that the electromagnetic fields they emit interfere constructively. The frequency range used in radiative heating systems typically operates between 70 and 120 MHz [34]. An additional method to effectively heat deep-seated tumors is by utilizing capacitive systems. This method requires one electrode to be placed on the patient while laying on the treatment bed and another electrode to be inserted. The electrodes are connected to a powerful generator that functions at frequencies from 8 to 40 MHz [35].



Figure 2.4: Two RF hyperthermia systems. Radiative-based BSD-2000 3D/MR (left) and Capacitive-based Thermotron RF-8EX (right)

Data obtained from: [35].

2.3.2 Superficial Local Hyperthermia

Superficial local HT is intended to treat tumors that are typically located within a maximum depth of 4 cm and specifically targets small and localized areas of the body such as lymph nodes in the head and neck region [35]. External devices such as antennas, capacitive electrodes or infrared lamps are used to deliver the proper treatment. Superficial HT uses antennas in the frequency range between 400 MHz and 1 GHz due to their effective energy deposition within 4 cm from the surface. The aim of the treatment is to develop different therapeutic outcomes by applying external heat. These outcomes consist of an increased vulnerability of malignant tumors to the alternative treatment methods, chemotherapy and radiation therapy as well as improved blood circulation to enhance the transportation of oxygen and essential nutrients to the specific area [35].

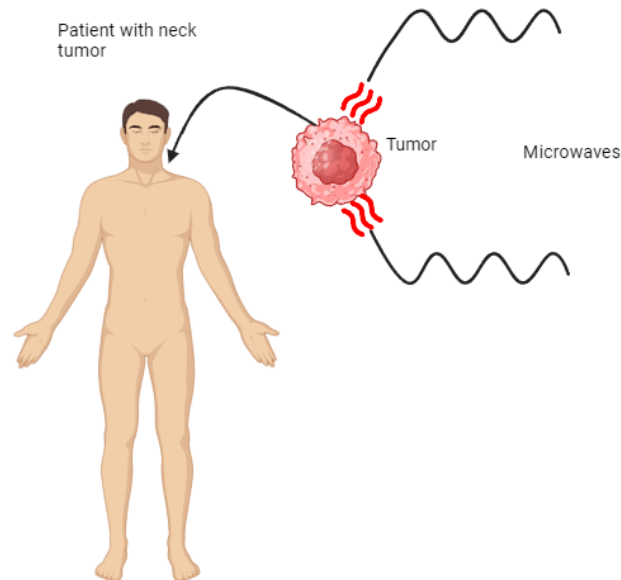


Figure 2.5: Superficial Hyperthermia Treatment
Created in Biorender.

2.4 Phantom Materials

The ongoing demand for tissue-like samples in the advancement of medical technology, along with the scarcity of human tissue due to ethical constraints, has resulted in the utilization of tissue models or phantoms that mimic the properties of human tissue [36]. The human body is a sophisticated system with distinct physical and electrical qualities present in all tissues. The main factor that contributes to the different dielectric properties of each tissue is the amount of water they consist of. Tissues such as muscle and brain exhibit high water content and other tissues, as those in fat and bone exhibit lower content of water in the body. In the past it was increasingly challenging to accurately represent all human tissue types due to the phantoms being mostly water-based. Currently more intricate phantoms are being developed to closely resemble human body tissues, including both heterogeneous and homogeneous phantoms [36].

2.4.1 Liquid Phantoms

In the early days of phantom development, most tissue-mimicking phantoms were liquid-based. Liquid phantoms is primarily used for high dielectric constant and lossy tissues, and is primarily used to mimic the optical properties of biological tissues. Water is the main component of the phantom composition to be able to mimic the higher dielectric properties. Other materials that are commonly utilized in liquid phantoms are agarose, glycerol, gelatin and polyvinyl alcohol [37]. Advantages of the water-based phantoms are the flexible and easy fabrication processes, high availability as well as low cost. Despite the easy and rapid fabrication process, liquid phantoms have a number of disadvantages. Due to the liquid nature of the phantom, a container or holder is required to carry the phantom. The container can be susceptible to mold growth, which can have an impact on the electrical properties of the phantom. Another disadvantage is the loss of water through evaporation from the phantom materials, leading to alterations in their properties as well as making them unsuitable for long-term preservation [36][40]. A blood-mimicking phantom, based on water, glycerol, salt and red dye (hemoglobin) can be implemented to simulate the dielectric properties of blood, in which the purpose of glycerol is to decrease the permittivity and salt to increase the conductivity [38].

Chemical Processes of Liquid Phantoms

The ability of liquid phantoms to flow and adapt to different shapes, makes them liquid-like. When glycerol is combined with water it dissolves relatively easy due to the hydrogen bonding between the water molecules and the hydroxyl groups of glycerol. Even though a chemical reaction does not take place, it helps to increase the viscosity of the solution, giving it mechanical qualities comparable to those of soft tissues [62]. Similarly, when gelatin is introduced to warm water, the protein chains start to hydrate and expand, causing the gelatin to dissolve. The viscosity and optical properties can then be adjusted by changing the gelatin concentration

[63]. When salt (e.g. NaCl) is dissolved in water it separates into positive sodium negative chloride ions. These ions typically increase the ionic strength of the solution and helps to adjust the electrical conductivity of the phantom to match those of biological tissues [64].

2.4.2 Semi-solid Phantoms

Phantoms that are semi-solid have capability to easily mold into any desired shape, while also possessing attributes that make them ideal for replicating the properties of soft tissues. Semi-solid materials can imitate both high and low permittivity tissues by employing materials such as agar, polyacrylamide and starch. Due to the lower water content opposed to liquid phantoms, semi-solid phantoms are typically reinforced with another polymer such as hydroxyethylcellulose or methylcellulose, developing a hydrogel, to be able increase its mechanical strength and durability [40]. Advantages of semi-solid phantoms are that they are more convenient to utilize and more efficient at simulating various tissues over a wide frequency range. Similar to liquid phantoms, they have good availability of materials with relatively low cost. While there are numerous advantages with semi-solid phantoms, there are also some disadvantages. Once the desired phantom is developed, its electrical properties can not be adjusted unlike liquid phantoms, where the permittivity can be increased further by adding water. The issue of evaporation and dehydration has also been observed to an extent with semi-solid phantoms, but not as severely as liquid phantoms. [40]. A semi-solid agar-based gel by Nilsson [39], included agar, sodium chloride and sugar dissolved in water, in which the purpose of sodium chloride was to adjust conductivity and sugar to achieve the desired permittivity.

Chemical Processes of Semi-Solid Phantoms

The gel-like consistency of semi-solid phantoms to maintain its shape like a solid and at the same time have viscoelastic properties similar to a liquid, renders them as semi-solid. [65]. When agar is dissolved in hot water (generally around 90°C), the agarose and agaropectin molecules combine to form a homogeneous solution. Upon cooling (under 40°C), agarose chains form a strong physical gel through hydrogen bonding. This produces a semi-solid gel, mimicking the stiffness of biological tissues such as muscle tissue [65]. Sugar on the other hand separates into two monosaccharides, glucose and fructose when dissolved in water. Similar to glycerol, a chemical reactions does not take place, but instead creates hydrogen bonds with water molecules, increasing the viscosity of the solution. Sugar may also assist in fine tuning the mechanical stiffness when mixed with agar [66].

2.4.3 Solid Phantoms

Solid tissue-mimicking phantoms, so called dry phantoms typically contain very small amounts of water, which allows them to avoid the evaporation issues associated with the other phantoms. Common materials used to develop solid phantoms are ceramic powder, silicone rubber, carbon fiber and graphite. The phantoms are mainly developed using ceramic powders, which are available in a diverse range of options and have a broad permittivity range. However, developing materials with high loss that can mimic the natural conductivity of tissues is difficult due to the low loss properties of ceramic materials [40][41]. Main advantages of solid phantoms is the evasion of evaporation and dehydration as well as sustaining durability to environmental changes opposed to other phantoms. Specialized equipment is necessary to produce solid materials due to the requirement of high temperatures in mixing the materials and high pressure in molding them. The use of specialized ceramic materials and instruments increases the cost of the fabrication process compared to other materials utilized in tissue-mimicking phantoms. Another disadvantage is that solid phantoms are difficult to reshape. This issue can however be addressed by introducing soft and dry materials, utilizing silicone rubber infused with carbon fiber, making the phantoms more stable and durable over time [40].

Chemical Processes of Solid Phantoms

In the development of solid phantoms, ceramic powders are commonly produced through sintering, which involves compacting and heating the powders to high temperatures without melting [67]. This permits the particles to bond together via diffusion processes, yielding a dense, solid structure. Under high pressure, the powder mixture is compressed into a mold, to produce a green body, which serves as a preliminary shape for the final phantom. The particles start to merge and densify when the green body is heated to a temperature below the heating point. This particular procedure can eliminate porosity, improving the phantom's mechanical qualities to make it solid-like [67].

2.5 Hydrogels in Hyperthermia Therapy

This section will discuss various polymers and hydrogels that were explored to develop the desired muscle phantom. The importance of parameters such as molecular weight, viscosity and concentration is also highlighted along with problems associated with air bubble formation during the phantom development procedure.

Hydrogels are polymer networks that are interconnected through crosslinking and have the ability to absorb large amounts of aqueous fluids. These materials are commonly characterized by their soft, flexible and biocompatible nature. Due to their high water content, porosity and softness, hydrogels typically exhibit properties that closely resemble those of living biological tissue, rendering them highly suitable for various medical applications, such as hyperthermia therapy [42].

2.5.1 Hydroxyethylcellulose

Hydroxyethylcellulose (HEC) is a water-soluble, nonionic gelling agent obtained from cellulose and primarily utilized as a thickening agent in phantom developments. Its potential as a hydrogel for hyperthermia applications is promising due to its distinctive characteristics and biocompatibility [40]. To successfully dissolve the polymer in water, HEC is commonly heated. It typically undergoes a phase transition from a homogeneous solution to a semi-solid, gel-like state when cooled down [44]. HEC offers several advantages:

Water Retention: HEC's ability to absorb and retain significant amounts of water is essential for maintaining hydration, but also preventing dehydration during hyperthermia therapies [44]. This feature ensures that the hydrogel maintains its properties, thus maximizing the efficacy of microwave energy absorption and heat production.

Mechanical Durability: HEC hydrogels can offer mechanical support and stability for phantoms during hyperthermia procedures, aiding in maintaining the intended shape of the hydrogel [44].

Biocompatibility: HEC being derived from cellulose, a naturally occurring polysaccharide present in plants, is generally regarded as biocompatible and non-toxic. This characteristic renders HEC hydrogels appropriate in phantom development for hyperthermia therapy, ensuring safety [44].

Chemical Process of Hydroxyethylcellulose

As hydroxyethylcellulose is introduced and dissolved in water, the water molecules start to hydrate. The hydroxyl groups in addition with the hydroxyethyl groups engage in the formation of hydrogen bonds with the water molecules [68]. Initially, the HEC particles undergo expansion as they absorb water. This leads to the penetration of water molecules into the polymer's structure, causing the individual polymer chains to swell and expand. As the swelling continues, the polymer chains start to disperse, spreading throughout the solution. This represents the dissolution process, during which HEC particles are fully solvated in water [68]. HEC is also known for its thickening properties, and typically increases the viscosity of the solution through the entanglement of the long polymer chains in water. The entanglement of the chains is responsible for the gel-like consistency and viscosity of HEC solutions [69].

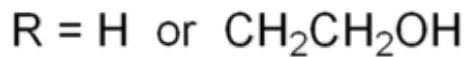
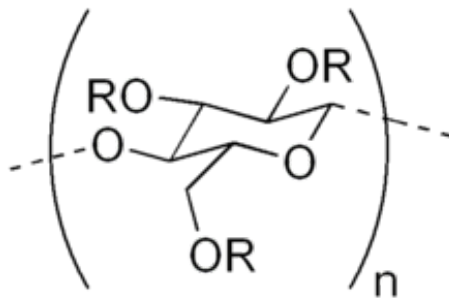


Figure 2.6: Structure of Hydroxyethylcellulose (HEC)
Data obtained from: [45].

2.5.2 Correlation between Molecular Weight, Viscosity and Concentration of HEC

To achieve a simple, rigid and durable phantom, it is important to find a balance between molecular weight (Mw), viscosity and concentration.

The viscosity of HEC solutions are affected by various elements, such as the concentration of HEC in the solution, the molecular weight as well as the degree of substitution (quantity of hydroxyethylcellulose groups per cellulose unit).

HEC with a greater molecular weight typically consists of lengthier polymer chains. Lengthier chains have a tendency to intertwine more easily and create a more tangled network structure within the solution. As mentioned before, this entanglement also results in an increased viscosity solution [44]. Furthermore, solutions with high molecular weight, are generally more viscous in comparison to those with lower molecular weight. The correlation is depicted in table 2.3 below.

HEC (Grade)	Molecular Weight (Da)	Viscosity (Room Temperature)	Concentration (%)
Natrosol L	90,000	75-150	5
Natrosol G	300,000	250-400	2
Natrosol M	720,000	4500-6500	2
Natrosol H	1,000,000	1500-2500	1
Natrosol HX	1,000,000	1500-2500	1
Natrosol HHX	1,300,000	3500-5500	1
Natrosol HHW	1,300,000	3500-5500	1

Table 2.3: Correlation between Molecular Weight, Viscosity and Concentration of HEC

Data obtained from [44].

The concentration of HEC in a solution is another crucial factor influencing the viscosity. An increase in the concentration of HEC results in a higher number of polymer chains per unit volume in the solution. The elevated polymer chain density promotes more frequent interactions among the chains, leading to increased entanglement and a higher viscosity of the solution [46]. Essentially, higher concentrations provide more opportunities for polymer chains to engage in interactions and establish a complex network structure, thereby enhancing the resistance to flow.

2.5.3 Methylcellulose

Another promising material that holds potential for application in phantoms is methylcellulose (MC). Methylcellulose is a cellulose ether derivative that exhibits semi-flexibility and is attributed to its capacity for solubilization in water [47]. MC is generally considered safe due to its non-toxic nature, biocompatibility and cost-effectiveness, making it a safe and efficient material to be utilized in tissue phantoms. Similar to HEC, MC-based hydrogels exhibit constrained durability over extended periods due to the phenomenon of thermal gelation. For lower molecular weights, MC necessitates the application of heat in order to undergo gelation, unlike HEC, which is capable of gel formation under cold conditions. However, this phenomenon is constrained when dealing with higher molecular weights. At similar molecular weights, MC is typically more viscous in comparison to HEC [48].

Chemical Process of Methylcellulose

Hydration is the first step that occurs when methylcellulose is dissolved in water. The water molecules are surrounded by the polymer chains and begins with the hydrophilic (water-attracting) parts [70]. The water molecules then force the polymer chains apart, causing them to swell as the chains hydrate. The swelling leads to an increase in viscosity, making the solution thicker. After hydration, the hydrogen bonds, holding the polymer chains together are broken by the water molecules penetrating the chains. This eventually causes methylcellulose to gradually disperse into the water [70].

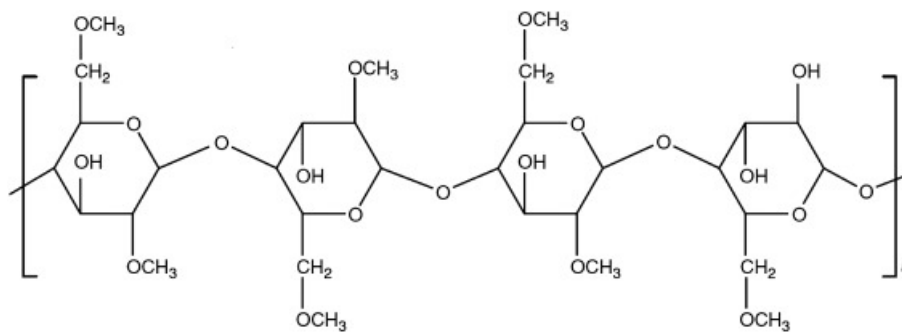


Figure 2.7: Structure of Methylcellulose (MC)

Data obtained from: [47].

2.5.4 Perfax (Methylcellulose-Based)

A methylcellulose-based powder, also called perfax, consisting of water, powder wallpaper paste and salt is of great interest. An advantage of this phantom is that it does not require heating for dissolution and can be used as reference phantom to develop a muscle phantom recipe, in order to evaluate the QA of deep regional hyperthermia [49]. Perfax is a type of powder adhesive based on polymers such as modified starch or methylcellulose and is initially synthesized as a wallpaper paste and wallcovering adhesives [50]. This powder is of great benefit to mimic the

dielectric properties of muscle tissue [46]. A limitation of the perfax phantom is the insufficient solidity. Its inadequate solidity causes it to behave fluidly at room temperatures, affecting the desired firmness and shape. As mentioned earlier, this attribution can have a connection to the specific molecular weight of MC utilized in the perfax powder.

2.5.5 Materials to Increase Mechanical Stability

Agar:

Agar is a polysaccharide that is naturally found in a number of red seaweeds, consisting of a combination of agarose and agaropectin. This hydrogel is a promising material due to its extraordinary thickening and gelling characteristics and can be combined with other hydrogels such as HEC to increase the gel's mechanical strength [51]. Agar gels exhibit outstanding thermal stability, enabling them to endure the elevated temperatures produced in microwave hyperthermia experiments without notable deterioration. Such stability plays a vital role in upholding the integrity of the phantom and ensuring the consistency of experimental outcomes [52]. Derived from natural origins, agar is widely recognized for its biocompatibility, rendering it suitable in phantom development [50]. The critical constraint of agar-based phantoms lies in their toughness, making them fragile and prone to breakage during handling as time passes [54].

Gelatin:

Another hydrogel that serves as a commonly used gelling agent in phantoms is gelatin. Gelatin consists of peptides, and proteins formed through the physical, thermal or chemical breakdown of collagen derived from various tissue such as skin, cartilage, tendon and bone [54]. The enduring stability over an extended period at room temperatures, cost-effectiveness, biocompatibility as well as easy manufacturing of gelatin-derived phantoms, render them appropriate for utilization in phantoms. A limitation of gelatin is its ability to sustain durable at elevated temperatures opposed to hydrogels such as agar/agarose [54].

2.5.6 Materials to Reduce Permittivity

Glycerol:

Glycerol is a compound found abundantly in nature and exists either in its free state or more commonly as an ester known as glycerides. It exhibits great versatility as a coupling agent due to its full miscibility in water, enabling customization of permittivity to suit a broad spectrum of tissue properties [55]. Glycerol has a lower dielectric constant (46.5) compared to water (80.1) [56]. This adaptability is particularly crucial in the context of phantom development, where achieving the desired permittivity is very important. Glycerol is considered to be optimal from a human safety standpoint due to its non-toxic nature and bacteria-static properties

[55].

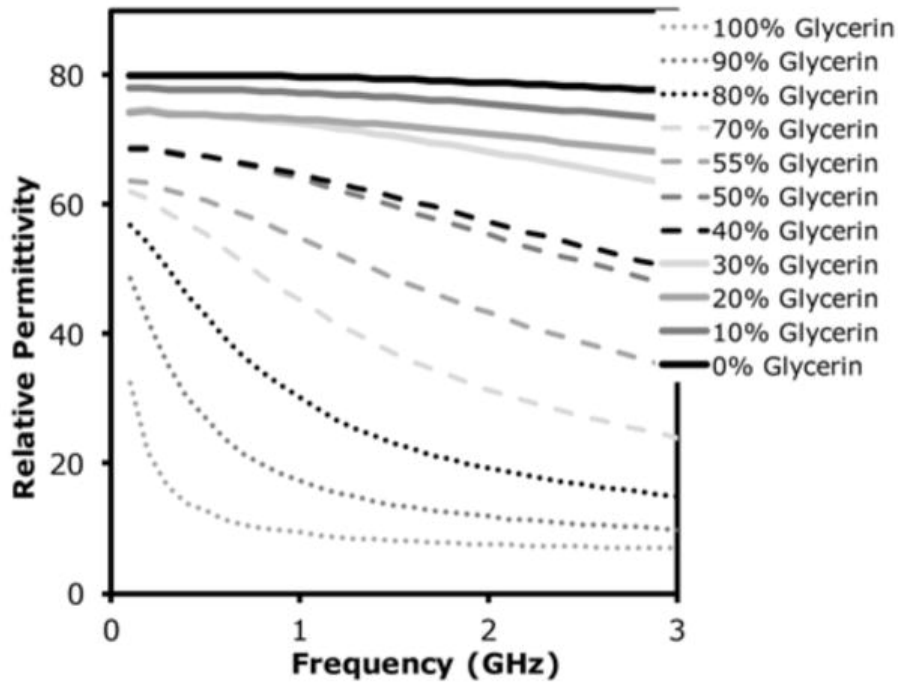


Figure 2.8: Measured Permittivity of Various Water/Glycerol Mixtures in relation to Frequency

Data obtained from: [55].

As seen in figure 2.8, the permittivity demonstrates a steady reduction as the glycerol concentration rises across all frequencies. A significant decrease in permittivity is observed at frequencies above 1 GHz [55].

Polyethylene Glycol:

Another material that can be used to reduce the permittivity of phantoms is polyethylene glycol (PEG). It is a synthetic polymer that is water-soluble, biocompatible and is widely utilized in the biomedical field. PEGs are typically available in a wide range of molecular weights, where they exhibit a liquid state below molecular weights of 600 Da and a solid state above 1000 Da [57]. PEG has a significantly lower dielectric constant compared to glycerol, and although it is typically more preferred to reduce the permittivity of phantoms, in terms of cost-effectiveness, the dielectric constant is very low and can affect other properties of the phantom as well. A limitation of utilizing PEG can be associated with the high molecular weights, typically leading to a very high viscosity as well as mixing difficulty [58].

2.5.7 Salt to Increase Conductivity

Sodium Chloride:

Sodium chloride, also called table salt, plays a pivotal role in phantom development, in the context of hyperthermia treatment. The human body exhibits a specific degree of electrical conductivity, due to the existence of electrolytes, such as potassium, sodium and chloride ions [59]. Through the incorporation of sodium chloride into the phantom, it is able to modify the conductivity in order to closely replicate that of human tissue. Sodium chloride is easily accessible, biocompatible and non-toxic at moderate concentrations as well as cost-effective, making it a viable option for adjusting conductivity in phantoms [59].

2.5.8 Occurrence of Air Bubbles in Phantoms

The mixing process of phantoms commonly induces the dissolution of air into the fluid, generally if the mixing is done above liquid level, and the presence of undischarged air may result in the formation of air bubbles in the final phantom. The elimination or reduction of the dissolved air is important due to the fact that air bubbles represent areas characterized by different optical attributes, such as zero scatter and absorption [60]. This can eventually impact the dielectric properties of the phantom and lead to inaccuracies in electrical assessments. If deviations are observed due to air bubbles, a vacuum chamber is typically used as an alternative to remove the bubbles [60].

3

Materials and Methods

This chapter seeks to describe the methods used in the development and assessment of muscle phantoms in MW HT. The material selection process is described, with an emphasis on the purpose of HEC, agar and glycerol in achieving the appropriate mechanical and dielectric properties. The phantom development procedure is discussed in detail, from material mixing to obtaining the gel phantom. Additionally, it includes the optimized recipes for different phantom compositions, aimed at specifically simulating the dielectric properties. This chapter further explains the setup used to assess the dielectric properties, including the equipment and measurement techniques.

3.1 Phantom Development Process

The phantoms were developed with the intention to be utilized solely as test samples and a total of 200 g phantom was developed for each phantom using a 250 ml glass beaker as a phantom holder. An exception was the perfax phantom, which was developed using a pot. As the perfax phantom could form a gel without heating, it did not require a water bath opposed to the HEC/Muscle phantom. In figure 3.1 the experimental setup and procedure can be observed for the muscle phantom. The pot is placed on a heating plate and is used as a water bath to be able to heat up the phantoms. As seen in the figure, the beaker is placed inside the water bath for heating and an overhead stirrer is placed inside the beaker for mixing. As HEC generally forms a gel when cooled down, 2/3 of the solution was heated to dissolve the powder and the remaining 1/3 was added after dissolution to form a gel. This process was performed based on the equipment that were available in the lab. With more advances equipment the method of procedure can be refined.

3.2 Material Selection

In the development of the muscle phantom, HEC is used as a base component that is dissolved in water. The use of higher molecular weights of HEC has been shown to be very promising to produce a mechanically stable gel, even at lower concentrations. It is readily dissolved in both hot and cold water and is biocompatible with a number of materials, making it a promising material. To further adjust the mechanical and dielectric properties of the gel phantom, three materials that are biocompatible with HEC are selected. Agar is employed as a gelling agent, that increases the gel's mechanical strength when combined with HEC. Agar is resistant

to high temperatures and is relatively firm at room temperature, which is important as the phantoms are stored at room temperature. To adjust the dielectric properties, permittivity and conductivity, glycerol and salt (NaCl) are employed. As the simulation of the permittivity is expected to be around 66.0, a material with a closer dielectric constant to that of water is preferred. Glycerol have a dielectric constant around 46, compared to polyethylene glycol, that have a much lower value, generally lower than 20, depending on the molecular weight. As glycerol have a value closer permittivity to that of water, it was preferred based on the materials available. Similarly, salt is utilized to increase the conductivity to the expected value of 0.71. The positive and negative ions of salt conducts electricity, when dissolved in water.



Figure 3.1: Experimental Setup and Procedure of Muscle Phantom

3.3 Phantom Development

3.3.1 Perfax Phantom

The perfax phantom serves as a benchmark for evaluating viscosity and solution thickness, making it ideal for comparative analysis. The amount utilized for each ingredient is necessary for the simulation of dielectric properties of muscle tissue at 100 MHz.

Ingredients	Amount
Perfax Powder	40 g
Salt (NaCl)	3,5 g
Water	1 L

Table 3.1: Ingredients of Perfax Phantom

Method of Procedure:

All ingredients are mixed at room temperature

1. 1 L of water is poured into a pot, followed by the addition of salt (NaCl).
2. Perfax powder is gradually added, as the solution is mixing, using an overhead stirrer.
3. Upon complete dissolution of the perfax powder without the presence of any lumps, the mixing process is complete.
4. The pot is sealed and stored at room temperature for approximately 24 h.

3.3.2 Hydroxyethylcellulose Gel

Hydroxyethylcellulose serves as a foundational element in the muscle phantom to guarantee the suitable levels of viscosity, thickness and firmness prior to the introduction of additional substances.

Three distinct HEC products are employed for experimental conditions with the aim of finding a balance between molecular weight and concentration of the final solution. As the higher molecular weights are generally limited to 2-3 wt%, the recipe illustrated in table 3.2 demonstrates a 2 wt% concentration to analyze the phantom solidity.

- (Hercules, Natrosol Plus)
- (Natrosol 250 M Pharm)
- (Natrosol 250 HHX Pharm)

Ingredients	Amount
Hydroxyethylcellulose (Natrosol)	4 g
Salt (NaCl)	0.7 g
Water	196 ml

Table 3.2: Ingredients of Hydroxyethylcellulose Phantom at 2 wt%

Method of Procedure: **All ingredients are mixed at elevated temperature**

1. A pot is positioned onto a heating plate, containing hot water. The hot water is intended to be used as a water bath. A thermometer is placed inside the water bath.
2. Of the total volume of water, two-thirds is transferred to a beaker and is subsequently immersed in the water bath. The remaining one-third is stored in a refrigerator.
3. Salt is introduced into the solution. The HEC powder is then gradually incorporated as the temperature rose, in order to avoid powder lumps and mixing difficulty. The solution is mixed using an overhead stirrer as the ingredients are added.
4. The HEC powder achieved complete dissolution without any visible aggregates in a temperature range of 60-70 °C of the water bath. As this temperature range appeared to be promising for full dissolution of HEC, it was used for the remaining experiments
5. To cool down the phantom, it is extracted from the water bath and the remaining one-third of stored water is gradually poured into the solution.
6. As the phantom cools down, it undergoes the gelation process and a homogeneous phantom is achieved.
7. The beaker is then sealed to avoid evaporation and possible contamination, and is stored at room temperature.

3.3.3 Muscle Phantom

To achieve the desired muscle phantom, the HEC phantom is combined with other promising materials, (agar and glycerol) to attain the envisioned dielectric and mechanical properties. Agar is incorporated into the solution in order to confer solidity upon the phantom. The introduction of glycerol served the purpose of reducing the permittivity, given the high dielectric constant of water.

Method of Procedure: All ingredients are mixed at elevated temperature

The procedure is very similar to that of the hydroxyethylcellulose phantom

1. A pot is positioned onto a heating plate, containing hot water. The hot water is intended to be used as a water bath. A thermometer is placed inside the water bath.
2. Of the total volume of water, two-thirds is transferred to a beaker and is subsequently immersed in the water bath. The remaining one-third is stored in a refrigerator.
3. Salt is introduced into the solution. The HEC powder is then gradually incorporated as the temperature rose, in order to avoid powder lumps and mixing difficulty. The solution is mixed using an overhead stirrer as the ingredients are added.
4. Once the HEC powder becomes perceptibly dissolved, glycerol is gradually added to the mixture.
5. As the solution starts to thicken, agar is added to the mixture in order to increase the solidity of the phantom.
6. The solution is subsequently agitated until the presence of aggregates is no longer visible. This is typically attained at a temperature range of 70-80 °C of the water bath.
7. To cool down the phantom, it is extracted from the water bath and the remaining one-third of stored water is gradually poured into the solution.
8. The phantom starts to solidify and hydrate as it cools down, and a homogeneous gel is achieved after a continuous 15-20 minutes of mixing.
9. The beaker is then sealed to avoid evaporation and possible contamination, and is stored at room temperature for further assessment of the dielectric properties.

3.3.3.1 Compositions of Muscle Phantom For The Optimized Recipes

	HEC 250 HHX (wt%)	Agar (wt%)	Glycerol (wt%)	Salt NaCl (g)
Phantom 1	2.5	1.5	16	0.7
Phantom 2	2.5	1.5	20	0.8
Phantom 3	2.5	1.5	25	1.0
Phantom 4	2.5	1.5	35	2.0
Phantom 5	2.5	1.5	40	1.4
Phantom 6	2.5	1.5	50	1.4

Table 3.3: Compositions For the Optimized Phantoms

The composition of the optimized phantoms are illustrated in table 3.3. To achieve the desired permittivity and conductivity of 66.0 and 0.71 of muscle tissue, both the glycerol and salt contents are optimized to analyze which phantom are at a closer proximity to the values. The HEC and agar content are definite to be able to have an accurate assessment. The content of both the materials were determined based on mixing difficulty, observation of the solidity as well as the amount of air bubbles generated after the gel is obtained.

To obtain a sufficient muscle phantom, the solidity and thickness of the phantom were analyzed by visually observing the properties using three distinct HEC products, varying in molecular weight. This assisted in finding a sufficient Mw for HEC. The assessment also requires the appropriate concentration of HEC, as very high concentrations often lead to mixing difficulty and undesired properties. Two factors are important when finding the suitable concentration, which will be assessed. One of them is the amount of air bubbles that is present at a particular concentration, and the other is the acquired solidity achieved. The amount of air bubbles that occurs in the phantom depends on a number of factors, such as the process of mixing as well as the rate of the mixer used. The air bubble formation will be analyzed by utilizing various mixing rates of the overhead mixer at the particular concentration chosen.

3.4 Dielectric Properties Assessment

The dielectric properties of the phantoms is assessed using the Dielectric Assessment Kit for Thin Layers (DAK-TL), connected to a Rohde & Schwarz ZNBT8 16 channels vector network analyzer. A phantom sample is put on a mechanically driven platform, which moves the sample toward the probe at the operator's specified force. The measuring device is managed by specific software installed on an external PC, which displays and saves the measurement data. To be able to analyze a wide range frequency of interest, two different probes are used: A red-marked probe, DAK12-TL2 (frequency range: 4-600 MHz), and a yellow-marked probe, DAK3.5-TL2 (frequency range: 200 MHz to 1 GHz). During each measurement, the phantom samples were further pushed toward the probe surface with a consistent force using the mechanically driven platform to ensure adequate phantom-probe contact. The permittivity and conductivity of each sample at the frequency range of interest can then be analyzed.

During the evaluation of the perfax phantom, the red-marked probe (DAK12-TL2) was used to analyze the permittivity and conductivity at the frequency range of 10-200 MHz. The yellow-marked probe, (DAK3.5-TL2) was utilized for the dielectric properties assessment of the hydroxyethylcellulose (HEC) phantoms at the frequency range of 200 - 490 MHz. During the assessment of the muscle phantom, the red-marked probe was yet again utilized, focusing on the frequency range spanning from 60-550 MHz. The primary object of the dielectric assessment is to replicate the standard values of muscle tissue at approximately 100 MHz.

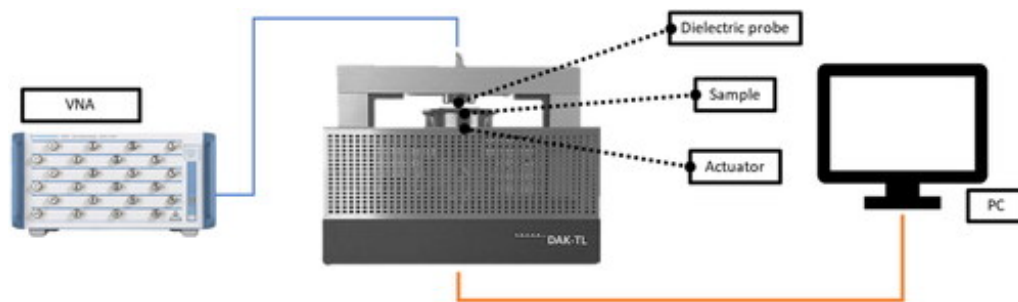


Figure 3.2: Schematic of the Measurement Setup for the Dielectric Properties (DAK-TL2)

Data obtained from [61].

4

Results & Discussion

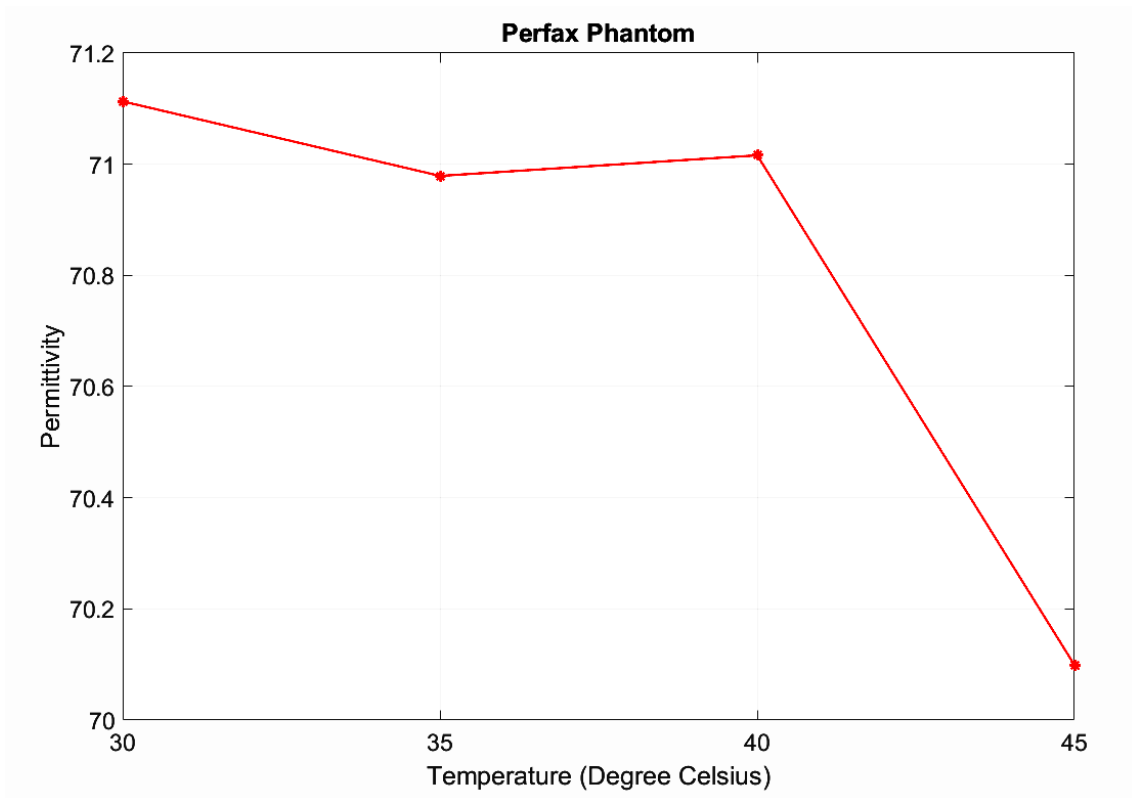
This chapter seeks to describe the results of the produced muscle phantoms, with a focus on the mechanical strength & dielectric properties. It starts by assessing the perfax phantom's properties at increased temperatures, providing information on its long-term stability. The chapter then discusses the optimization of the muscle phantoms, including the analysis of HEC concentration, air bubble formation and the mechanical properties of the phantoms. Finally, it assesses the dielectric properties and compares them with the target values for muscle tissues, highlighting the significance of the results.

4.1 Dielectric Properties of Perfax Phantom at Elevated Temperatures

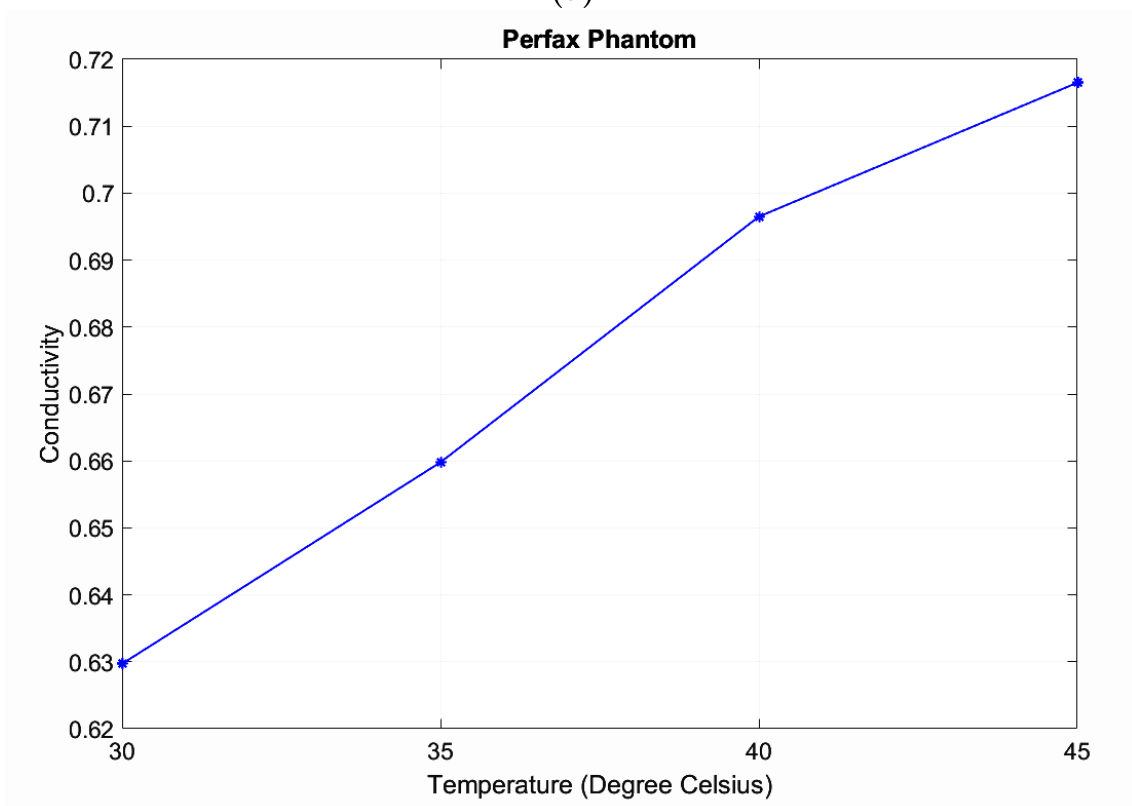
In figure 4.1, the graph in a) represents the change in permittivity at elevated temperatures (30-45 °C), and b) denotes the change in conductivity. As the experiment was conducted 3 weeks after phantom development, minor deviations are observed in both permittivity and conductivity from their expected values.

The purpose of the experiment is to observe the change in dielectric properties at elevated temperatures intended for treating deep-seated tumors. As illustrated in the graphs, the permittivity decreases with an increase in temperature, whereas the conductivity exhibits a rising trend. The variations observed within the temperature range are deemed not substantial, leading to the inference that alterations in temperature of the phantom does not exert a significant influence on its properties.

The y-axis represents the a) permittivity, b) conductivity and the x-axis represents the temperature (°C).



(a)



(b)

Figure 4.1: a) Permittivity at Elevated Temperatures b) Conductivity at Elevated Temperatures

4.2 Phantom Process Optimization

4.2.1 Analysis of HEC Gel Solidity

HEC (Product)	Viscosity	Solidity
Hercules, Natrosol Plus	Low	Low
Natrosol 250 M Pharm	Moderate	Moderate
Natrosol 250 HHX Pharm	High	Moderate

Table 4.1: Viscosity of HEC Products, Differing in Mw

Three HEC products, differing in molecular weights were examined in order to investigate the viscosity and consistency of the resulting phantom gel. As seen in table 4.2, the distinct products exhibited various viscosity concentrations and solidity. This confirms that higher molecular weights of polymers typically leads to higher viscosity of the resulting gel. Similarly, Higher molecular weights seem to increase the solidity of the gel as well. When finding a balance in molecular weight, it is also important to consider mixing difficulty, to avoid formation of lumps and aggregates in the solution. A visual observation of the phantom solutions determined that the HEC formulation, Natrosol 250 HHX Pharm exhibited a denser texture in comparison to the Natrosol 250 M Pharm product due to its elevated molecular weight, thus warranting its selection for subsequent investigative procedures.

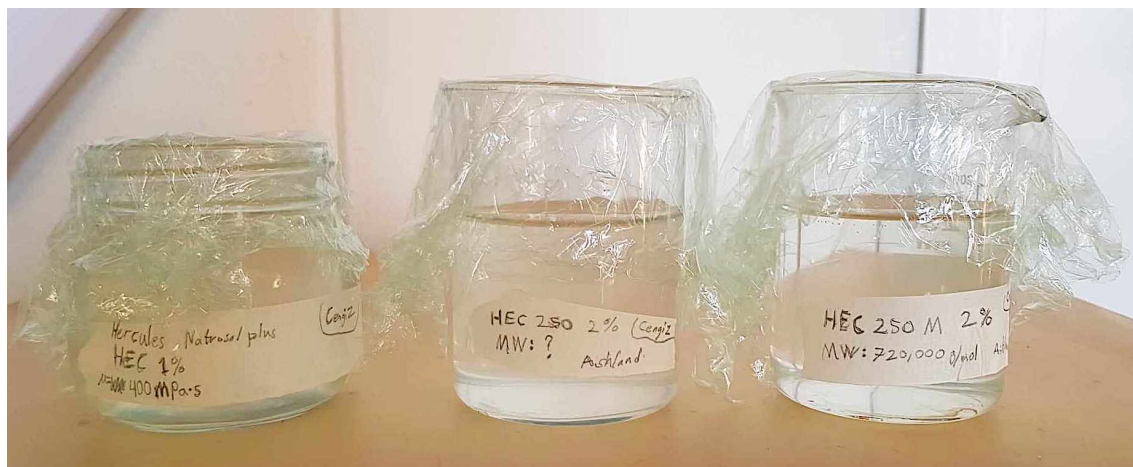


Figure 4.2: HEC Gels, Each Containing Distinct Molecular Weights

4.2.2 Analysis of HEC Gel Concentration

In order to achieve a rigid gel, and avoid mixing difficulty as well as the formation of air bubbles in the final muscle phantom, adequate concentration levels are required. The HEC product, Natrosol 250 HHX Pharm is utilized for the concentration assessment.

Concentration of HEC (Natrosol 250 HHX)	Air Bubbles (Amount)	Solidity
3wt%	No	Moderate
3.5wt%	Few	Moderate
4wt%	High	High

Table 4.2: Air Bubbles and Solidity assessment of HEC at Various Concentrations

From the data presented in table 4.3, one can discern that higher levels of HEC, lead to an increased formation of air bubbles within the resulting gel. The firmness of the gel also appears to rise as a result of enhanced interweaving and linking of polymer chains. Despite the fact that a 4wt% HEC facilitated the attainment of the desired solidity in the phantom, a noticeable quantity of air bubbles persisted, a factor that is important to eliminate in order to achieve an accurate dielectric assessment. In most instances, a minimal number of small air bubbles in gel phantoms typically have negligible effects on their properties, hence the concentration of 3.5wt% HEC emerged as the most suitable option to strike a balance between solidity and the presence of air bubbles.



Figure 4.3: Phantom Appearance of Natrosol 250 HHX at Various Concentrations: Left: 3wt% to Right: 4wt%

4.2.3 Air Bubbles Formation Assessment

The process of mixing plays a pivotal role in attaining a consistent and even distribution of HEC within the gel. The speed at which the mixer is employed often influences both the quantity and size of air bubbles generated within the solution as a result of the incorporation of air. An assessment of the HEC gel is conducted across different mixing velocities to examine the effects on air bubble formation.

HEC (3.5wt%)	Overhead Mixer (rpm)	Temperature of Water Bath (Celsius)
Gel 1	200 -> 400 -> 600 -> 200	64
Gel 2	400 -> 600 -> 800 -> 400	60
Gel 3	600 -> 800 -> 1000 -> 600	62

Table 4.3: Quantity and Size of Air Bubbles at Different Mixing Rates

The mixing velocities for each phantom were observed 3 days after development according to table 4.4. The velocity values indicate the values at which the mixing rate was initiated, then steadily escalated to prevent the formation of lumps, and eventually reverted to the original starting value upon cooling down of the gel. This assessment has validated that reduced velocity levels of the overhead mixer led to a decreased presence of air bubbles compared to elevated mixing rates as observed with "Gel 1". This phenomenon is primarily attributed to a lesser amount of air being incorporated into the solution during phantom development. There are instances where a higher mixing speed may be preferred for the production of different kinds of phantoms with lower viscosity, mainly for reasons related to time effectiveness and an expedited mixing procedure.



Figure 4.4: Phantom Appearance of Natrosol 250 HHX at Various Mixing Velocities: Left: Phantom 1 to Right: Phantom 3

4.2.4 HEC Gel Confirmation

To validate the consistent physical resemblance achieved in gel 1, three additional HEC gels were produced utilizing identical composition and procedural methodology. This is crucial to ensure that identical features of the gel are obtained using the same recipe.

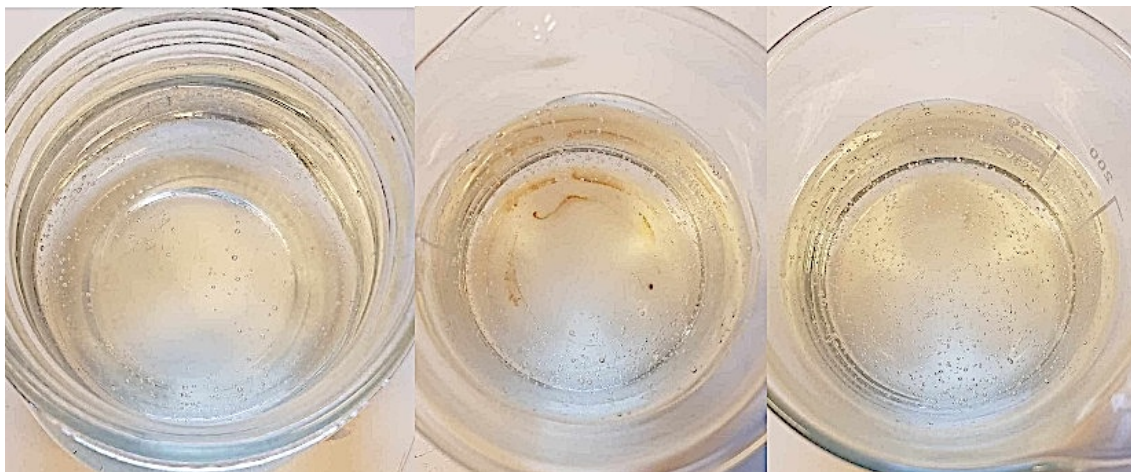


Figure 4.5: Gel Appearance of Natrosol 250 HHX: Left: Gel 1 to Right: Gel 3

From figure 4.5, it is evident that the HEC gels exhibited a noticeable resemblance to "Gel 1" as per the previous analysis. The gels denoted as 2 and 3 displayed a marginally higher presence of air bubbles in contrast to gel 1, a factor that may vary with time. With the progression of time, these bubbles are expected to gradually ascend to the surface and dissipate. This analysis provides additional evidence supporting the assertion that decreased rates of the overhead mixer lead to a decline in both the size and quantity of air bubbles within the solution.

4.3 Dielectric Properties Assessment

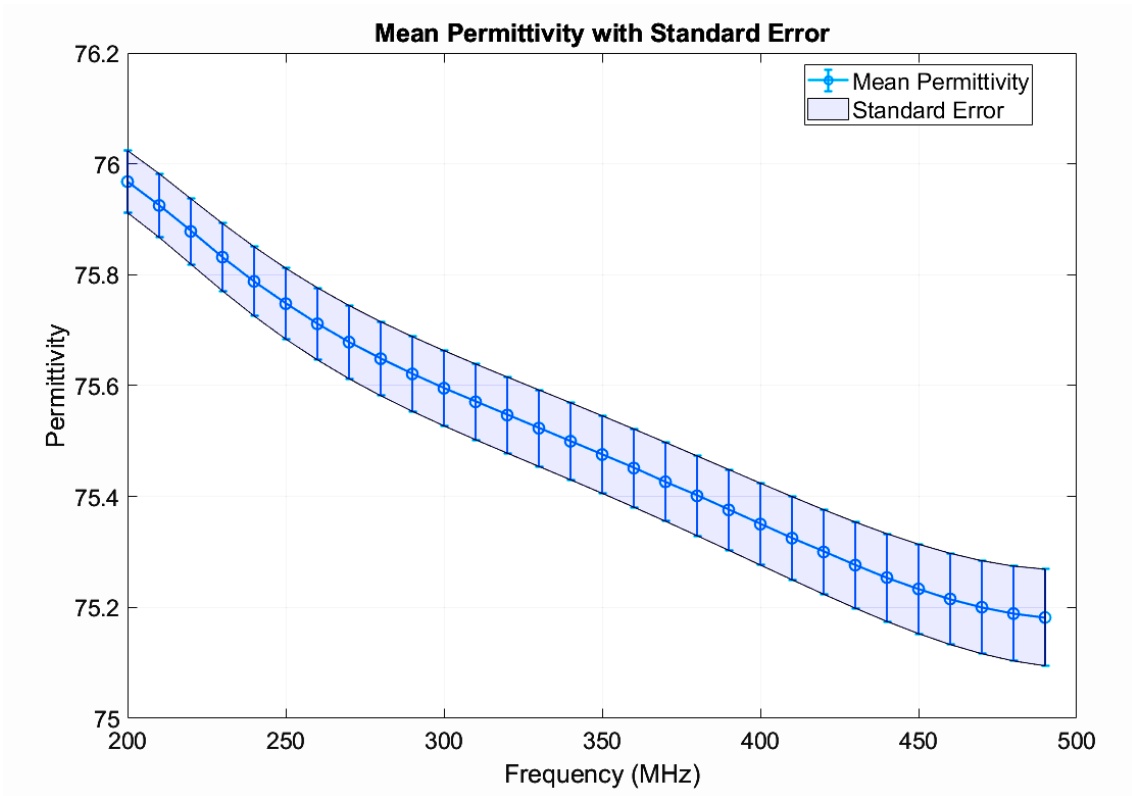
4.3.1 Dielectric Properties (Mean & Deviation) of HEC Gels

In order to assess the distinctions and variations among the HEC gel properties using the same recipe, the average values as well as the standard deviation of the dielectric characteristics were observed.

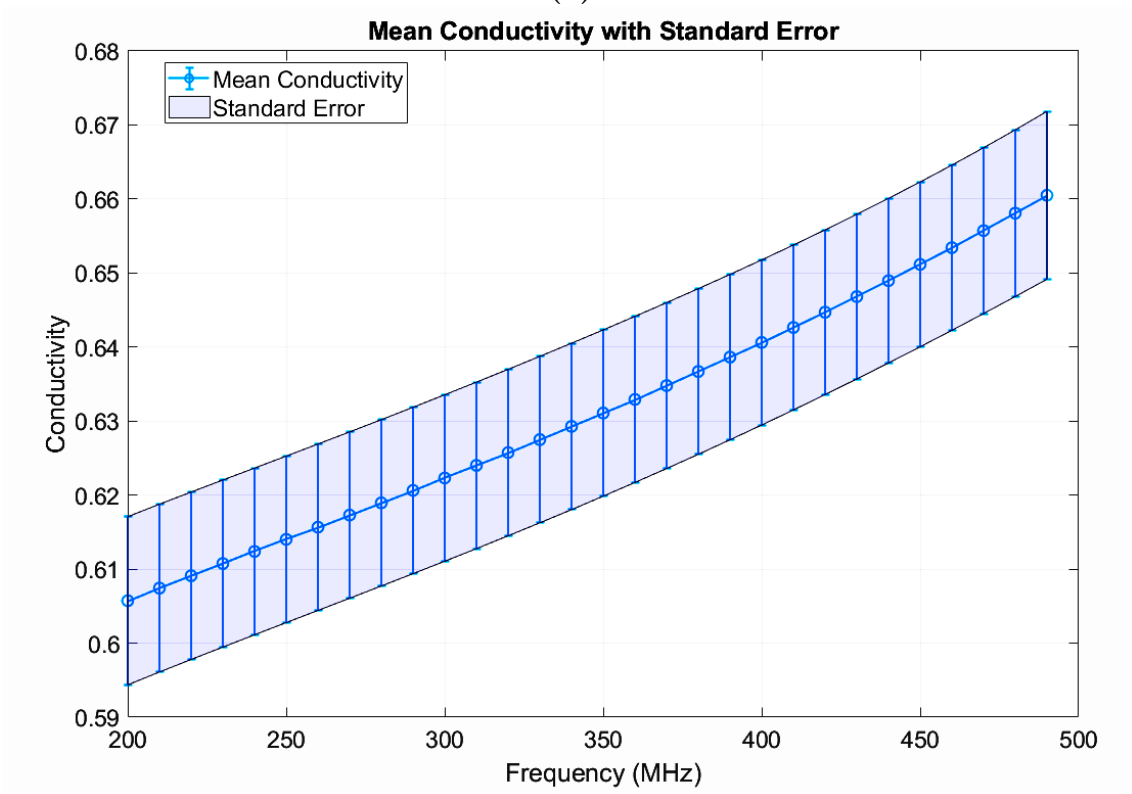
In figure 4.6 depicted below, the mean permittivity and conductivity of the three HEC gels are observable alongside their respective measurement uncertainties. The blue line illustrates the mean values, while the shaded area denotes the standard deviations from the mean. This analysis holds significance in ensuring the absence of significant differences among the phantoms concerning their dielectric properties based on the same recipe. Frequencies exceeding 100 MHz commonly exhibit uncertainties that may extend up to 15%, whereas frequencies below 100 MHz typically range around 5%. As depicted in a), there are no significant deviations from the mean permittivity values. The most notable discrepancy spans from 75.1 to 76.02, corresponding to an approximate 1.2% uncertainty. This validation indicates that all permittivity values fall within the 5% uncertainty requirement.

In b), the shaded region appears to be broader, indicating a higher uncertainty. The largest deviation spans from 0.595 to 0.672, resulting in a 13% error rate. This suggests that one of the phantoms manifested a higher conductivity in comparison to the other two phantoms. Given that salt (NaCl) is recognized for its substantial influence on conductivity, the presence of a measurement or experimental error is conceivable.

The y-axis represents the a) permittivity, b) conductivity, and the x-axis represents the frequency range.



(a)



(b)

Figure 4.6: a) Average Permittivity along with Standard Deviation Over the Frequency Range (200-490 MHz) b) Average Conductivity along with Standard Deviation Over the Frequency Range (200-490 MHz)

4.3.2 Dielectric Properties of Muscle Phantoms

The graph in figure 4.8 a) below illustrates the optimized recipes outlined in table 3.3. In order to achieve the targeted permittivity at 100 MHz, adjustments were made to the glycerol component. The various coloured lines depicted in a) correspond to the differing levels of glycerol content that were employed. Specifically, the uppermost blue line is denoted as "16Gly", signifying the utilization of 16% glycerol in the phantom composition. Based on the graph, it is evident that the black line (35Gly) and the purple line (40Gly) exhibit permittivity values (65&67) very proximate to the desired permittivity (66) of muscle tissue as specified in table 2.1 at 100 MHz. Given that both lines demonstrate a deviation error within 5% of the target value, the glycerol content falling within the range 35-40% emerges as a viable range for mimicking the permittivity.

To replicate the intended conductivity of muscle tissue (0.71), as specified in table 2.2 at 100 MHz, two "35Gly" phantoms can be observed in b). The red line exhibits a greater conductivity (0.63) in comparison to the blue line (0.57) which is closer to the target value. Despite surpassing the 5% margin of error, a slight elevation in salt concentration could enable the attainment of the desired conductivity.

The y-axis represents the a) permittivity, b) conductivity, and the x-axis represents the frequency range.

Muscle Phantom	Salt (NaCl) Content (g)
35Gly(1) - Red Line	2.0 g
35Gly(2) - Blue Line	1.7 g

Table 4.4: Composition of Muscle Phantom Illustrated in Graph 4.8 b)



Figure 4.7: Final Muscle Phantom (Produced from Phantom Recipe 4)

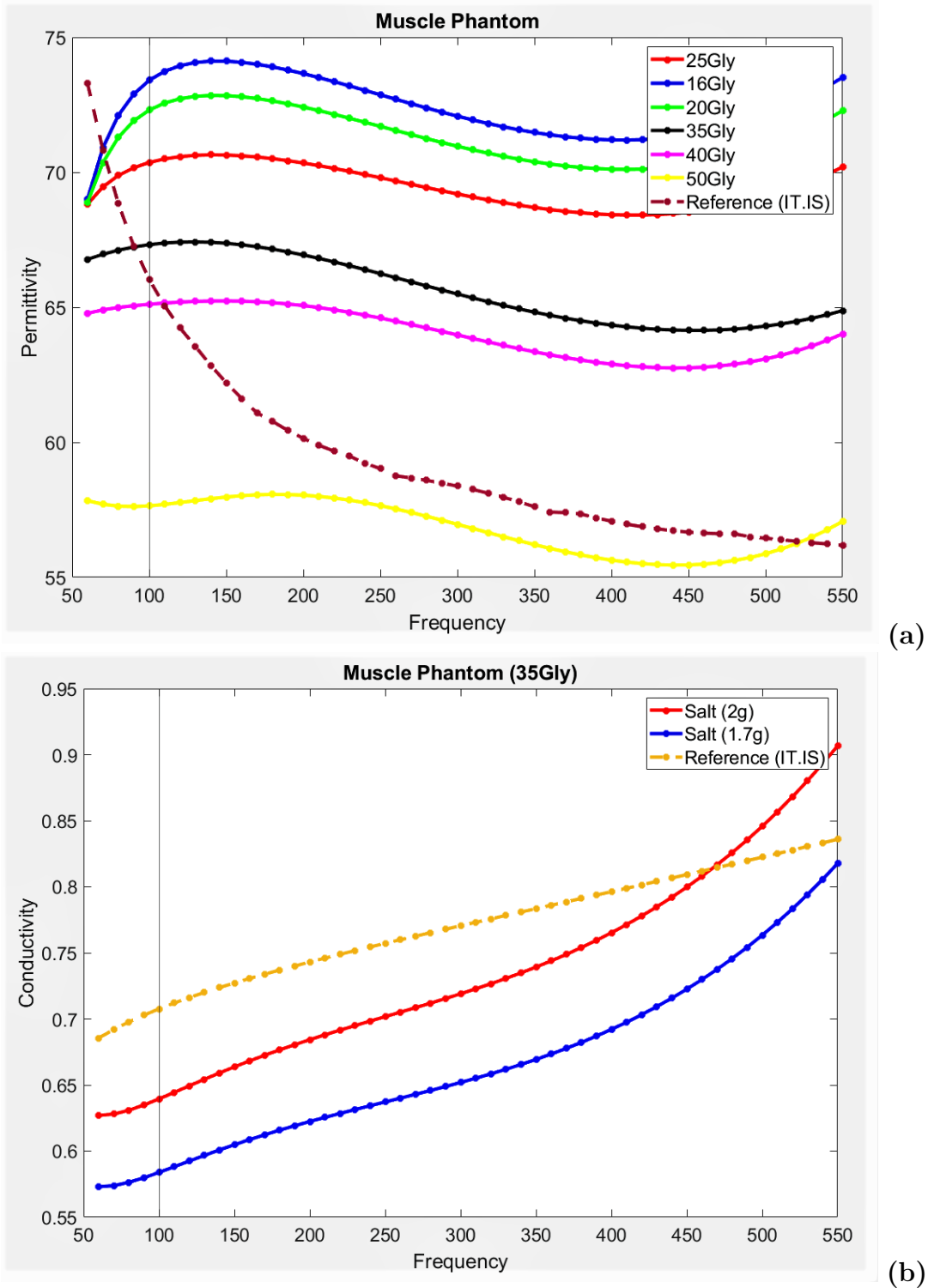


Figure 4.8: **a)** Permittivity of the Optimized Phantom Recipes Over the Frequency Range (60-550 MHz) **b)** Conductivity of Two 35Gly Phantoms Over the Frequency Range (60-550 MHz)

5

Conclusion/Future Outlook

This study has examined a variety of materials, compositions and parameters in order to develop a homogeneous muscle phantom that functions effectively, designed to evaluate the efficacy of heating devices. The developed muscle phantom demonstrated satisfactory mechanical strength through the utilization of hydroxyethylcellulose as primary component and agar to enhance the phantom's durability. In the treatment of deep-seated tumors, devices that operate at frequencies lower than 120 MHz are commonly favored, making the simulation of dielectric properties at 100 MHz an important consideration. Given the high permittivity of water, glycerol was employed to reduce the permittivity, while salt (NaCl) was added to increase the conductivity of the phantom solution. The muscle phantom managed to closely imitate the dielectric characteristics at 100 MHz with an error of margin within 5%, and displayed decent firmness.

In comparison with other phantoms, such as the perfax phantom, the produced muscle phantom was shown to be solid at room temperature with viscoelastic properties, while the perfax phantom formed a relatively weak gel and was very viscous at the same temperature. The solid feature of the muscle phantom can be attributed to the use of high viscosity and molecular weight of hydroxyethylcellulose combined with the thickening agent of agar. In contrast to other semi-solid phantoms (agar-based phantoms), the muscle phantom can be durable and stable in the long-term due to the hydrophilic properties of hydroxyethylcellulose, reducing the rate of evaporation. Agar-based phantoms are more firm initially, but will become brittle and degrade with time.

In conclusion, the development of a mechanically stable gel phantom that replicates the properties at approximately 100 MHz has shown to be successful, with the aim to aid in the treatment of deep regionally located tumors in the human body using electromagnetic radiation to generate heat.

Further investigation of the developed muscle phantom can be necessary to guarantee its efficient utilization as a phantom. The final phantom was fabricated using the accessible equipment available. Using more sophisticated equipment for production could be conducted to observe any disparities in the quality of the phantom. The examination of the phantom's longevity and storage duration can be accurately conducted by observing the variations in its dielectric properties over an extended time-period. This procedure can ascertain the duration for which the phantom remains suitable for evaluating the efficacy of heating devices, with respect to both

5. Conclusion/Future Outlook

quality and safety. Additionally, subjecting the phantom to elevated temperatures can facilitate an analysis of its solidity and alterations in properties to validate the phantom's suitability as a test object.

Bibliography

- [1] WHO, "Cancer", Jan. 2024.
<https://www.who.int/health-topics/cancer#tab=tab-1>
- [2] National Cancer Institute, "What is Cancer", Oct. 2021.
<https://www.cancer.gov/about-cancer/understanding/what-is-cancer>
- [3] Cleveland Clinic, "Tumor", Oct. 2021.
<https://my.clevelandclinic.org/health/diseases/21881-tumor>
- [4] WHO, "Cancer Today", Feb. 2024.
<https://gco.iarc.fr/today/en/dataviz/pie?mode=population&group-populations=0>
- [5] American Society of Clinical Oncology, "Progress Against Cancer", Feb 2024.
<https://www.cancer.net/sites/cancer.net/files/vignette/Progress-Against-Cancer-Timeline.pdf>
- [6] Salihi A, Al-Naqshabandi MA, Khudhur ZO, Housein Z, Hama HA, Abdullah RM, Hussen BM, Alkasalias T. Gasotransmitters in the tumor microenvironment: Impacts on cancer chemotherapy (Review). *Mol Med Rep*. 2022.
- [7] Cancer Research UK, "What is cancer surgery", May. 2022.
<https://www.cancerresearchuk.org/about-cancer/treatment/surgery/about>
- [8] M.R. Horsman, J. Overgaard. Hyperthermia: a Potent Enhancer of Radiotherapy, *Clinical Oncology*, Volume 19, Issue 6, 2007, Pages 418-426, ISSN 0936-6555.
- [9] Yi GY, Kim MJ, Kim HI, Park J, Baek SH. Hyperthermia Treatment as a Promising Anti-Cancer Strategy: Therapeutic Targets, Perspective Mechanisms and Synergistic Combinations in Experimental Approaches. *Antioxidants* (Basel). 2022 Mar 24;11(4):625.
- [10] Cheng Y, Weng S, Yu L, Zhu N, Yang M, Yuan Y. The Role of Hyperthermia in the Multidisciplinary Treatment of Malignant Tumors. *Integr Cancer Ther*. 2019 Jan-Dec;18:1534735419876345.
- [11] Rao W, Deng ZS, Liu J. A review of hyperthermia combined with radiotherapy/chemotherapy on malignant tumors. *Crit Rev Biomed Eng*. 2010;38(1):101-16.
- [12] M.M. Paulides, H. Dobsicek Trefna, S. Curto, D.B. Rodrigues, Recent technological advancements in radiofrequency- and microwave-mediated hyperthermia for enhancing drug delivery, *Advanced Drug Delivery Reviews*, Volumes 163–164, 2020, Pages 3-18, ISSN 0169-409X.

- [13] Government of Canada, "Limits of Human Exposure to Radiofrequency Electromagnetic Energy in the Frequency Range from 3kHz to 300 GHz", Aug. 2019.
<https://www.canada.ca/en/health-canada/services/publications/health-risks-safety/limits-human-exposure-radiofrequency-electromagnetic-energy-range-3-300.html>
- [14] Iowa State University, "Frequency Spectrum of Microwave and Millimeter Waves", Feb. 2024.
<https://www.nde-ed.org/NDETechniques/Microwaves/Introduction/Other.xhtml>
- [15] Eranki A, Mikhail AS, Negussie AH, Katti PS, Wood BJ, Partanen A. Tissue-mimicking thermochromic phantom for characterization of HIFU devices and applications. *Int J Hyperthermia*. 2019;36(1):518-529.
- [16] Scutigliani EM, Liang Y, Crezee H, Kanaar R, Krawczyk PM. Modulating the Heat Stress Response to Improve Hyperthermia-Based Anticancer Treatments. *Cancers (Basel)*. 2021 Mar 12;13(6):1243.
- [17] Bakker, A., van der Zee, J., van Tienhoven, G., Kok, H. P., Rasch, C. R. N., & Crezee, H. (2019). Temperature and thermal dose during radiotherapy and hyperthermia for recurrent breast cancer are related to clinical outcome and thermal toxicity: a systematic review. *International Journal of Hyperthermia*, 36(1), 1023–1038.
- [18] International Standard Organization, "Quality assurance: A critical ingredient for organizational success", Mar. 2024.
<https://www.iso.org/quality-management/quality-assurance>
- [19] M. De Lazzari, W. Napieralski, T. Nguyen, A. Ström and H. D. Trefná, "Design and manufacture procedures of phantoms for hyperthermia QA guidelines," 2023 17th European Conference on Antennas and Propagation (EuCAP), Florence, Italy, 2023, pp. 1-5.
- [20] American Association of Physicists in Medicine, "Dielectric properties of colon polyps, cancer, and normal mucosa: Ex vivo measurements from 0.5 to 20 GHz", May. 2018.
<https://aapm.onlinelibrary.wiley.com/doi/10.1002/mp.13016>
- [21] Griffiths, David J. *Introduction to Electrodynamics*. 4th ed., Pearson, 2013.
- [22] Malmivuo, Jaakko, and Robert Plonsey. *Bioelectromagnetism: Principles and Applications of Bioelectric and Biomagnetic Fields*. Oxford University Press, 1995.
- [23] Farrugia. L, Porter. E, Di Meo. S. *IEEE Access*, "The complex permittivity of biological tissues: a practical measurement guideline", Jan. 2024.
- [24] Gabriel. C, "The Dielectric Properties of Tissue", Mar. 2024.
https://link.springer.com/content/pdf/10.1007/978-94-011-4191-8_10.pdf?pdf=inline%20link
- [25] TeachMe Anatomy, "Ultrastructure of Skin", Feb. 2022.
<https://teachmeanatomy.info/the-basics/ultrastructure/skin/>
- [26] Miklavčič, Damijan, Natasa Pavselj and Francis X. Hart. "ELECTRIC PROPERTIES OF TISSUES." Apr. (2006).
- [27] Kittel, C. (2005). *Introduction to Solid State Physics* (8th ed.). Wiley.

-
- [28] C. Gabriel. Compilation of the Dielectric Properties of Body Tissues at RF and Microwave Frequencies, Report N.AL/OE-TR- 1996-0037, Occupational and environmental health directorate, Radiofrequency Radiation Division, Brooks Air Force Base, Texas (USA), 1996.
<https://itis.swiss/virtual-population/tissue-properties/database/dielectric-properties>
- [29] National Library of Medicine, "Non-Ionizing Radiation, Part 2: Radiofrequency Electromagnetic Fields", 2013.
<https://www.ncbi.nlm.nih.gov/books/NBK304634/>
- [30] IEEE Standard for Safety Levels with Respect to Human Exposure to Radio Frequency Electromagnetic Fields, 3 kHz to 300 GHz," in IEEE Std C95.1-2005 (Revision of IEEE Std C95.1-1991) , vol., no., pp.1-238, 19 April 2006, doi: 10.1109/IEEESTD.2006.99501.
- [31] Gabriel, C., Gabriel, S., & Corthout, E. (1996). "The Dielectric Properties of Biological Tissues: I. Literature Survey." *Physics in Medicine and Biology*, 41(11), 2231-2249.
- [32] Bhargava, D. Leeprechano, N. Rattanadecho, P. Wessapan, T. Specific absorption rate and temperature elevation in the human head due to overexposure to mobile phone radiation with different usage patterns, *International Journal of Heat and Mass Transfer*, Volume 130, 2019, Pages 1178-1188, ISSN 0017-9310, <https://doi.org/10.1016/j.ijheatmasstransfer.2018.11.031>.
- [33] American Cancer Society. "Hyperthermia to Treat Cancer", May. 2016.
<https://www.cancer.org/cancer/managing-cancer/treatment-types/hyperthermia.html>
- [34] Kok, H. P., Navarro, F., Strigari, L., Cavagnaro, M., & Crezee, J. (2018). Locoregional hyperthermia of deep-seated tumours applied with capacitive and radiative systems: a simulation study. *International Journal of Hyperthermia*, 34(6), 714–730. <https://doi.org/10.1080/02656736.2018.1448119>
- [35] M.M. Paulides, H. Dobsicek Trefna, S. Curto, D.B. Rodrigues, Recent technological advancements in radiofrequency- and microwave-mediated hyperthermia for enhancing drug delivery, *Advanced Drug Delivery Reviews*, Volumes 163–164, 2020, Pages 3-18, ISSN 0169-409X, <https://doi.org/10.1016/j.addr.2020.03.004>.
- [36] Vardaki MZ, Kourkoumelis N. Tissue Phantoms for Biomedical Applications in Raman Spectroscopy: A Review. *Biomedical Engineering and Computational Biology*. 2020;11. doi:10.1177/1179597220948100
- [37] Luciana C Cabrelli et al 2017 *Phys. Med. Biol.* 62 432. doi: 10.1088/1361-6560/62/2/432
- [38] Samavat H, Evans JA. An ideal blood mimicking fluid for doppler ultrasound phantoms. *J Med Phys.* 2006 Oct;31(4):275-8. doi: 10.4103/0971-6203.29198. PMID: 21206644; PMCID: PMC3004103.
- [39] Nilsson P. 1984. Physics and technique of microwave-induced hyperthermia in the treatment of malignant tumors. PhD thesis. University of Lund, Lund.

- [40] A. T. Mobashsher and A. M. Abbosh, "Artificial Human Phantoms: Human Proxy in Testing Microwave Apparatuses That Have Electromagnetic Interaction with the Human Body," in *IEEE Microwave Magazine*, vol. 16, no. 6, pp. 42-62, July 2015, doi: 10.1109/MMM.2015.2419772.
- [41] K. Ito, K. Furuya, Y. Okano and L. Hamada: "Development and the Characteristics of a Biological Tissue-equivalent Phantom for Microwaves," *IEICE Trans*, Vol. J81-B-II, No. 12, pp. 1126-1135, Dec. 1998(in Japan).
- [42] Shuoxuan Wang, Yuping Wei, Yong Wang, Yue Cheng, Cyclodextrin regulated natural polysaccharide hydrogels for biomedical applications-a review, *Carbohydrate Polymers*, Volume 313, 2023,120760, ISSN 0144-8617, <https://doi.org/10.1016/j.carbpol.2023.120760>.
- [43] Dabbagh, Ali & Abdullah, Bjj & Ramasindarum, Chanthiriga & Abu Kasim, Noor. (2014). Tissue-Mimicking Gel Phantoms for Thermal Therapy Studies. *Ultrasonic imaging*. 36. 10.1177/0161734614526372.
- [44] Ashland. "formulating elegant liquid and semisolid drug products", *natrosol 250 hydroxyethylcellulose (HEC)*. 2018.
- [45] The Cosmetic Chemist. "Hydroxyethylcellulose", 2016. http://www.thecosmeticchemist.com/molecule_of_the_week/hydroxyethylcellulose.html
- [46] K Benyounes et al 2018 *J. Phys.: Conf. Ser.* 1045 012008.
- [47] Supaluck Kraithong, Atiruj Theppawong, Suyong Lee, Riming Huang, "Understanding of hydrocolloid functions for enhancing the physicochemical features of rice flour and noodles", *Food Hydrocolloids*, Volume 142, 2023, 108821, ISSN 0268-005X, <https://doi.org/10.1016/j.foodhyd.2023.108821>.
- [48] Simone S. Stalling, Sunday O. Akintoye, Steven B. Nicoll, Development of photocrosslinked methylcellulose hydrogels for soft tissue reconstruction, *Acta Biomaterialia*, Volume 5, Issue 6, 2009, Pages 1911-1918, ISSN 1742-7061, <https://doi.org/10.1016/j.actbio.2009.02.020>.
- [49] Farina L, Sumser K, van Rhoon G, Curto S. Thermal Characterization of Phantoms Used for Quality Assurance of Deep Hyperthermia Systems. *Sensors (Basel)*. 2020 Aug 13;20(16):4549. doi: 10.3390/s20164549. PMID: 32823788; PMCID: PMC7472229.
- [50] Henkel. *Perfax Powder*. Apr. 2024. <https://www.henkel.com/our-businesses/perfax-691040>
- [51] Ana M.M. Sousa, Cristina M.R. Rocha, Maria P. Gonçalves, Chapter 24 - Agar, Editor(s): Glyn O. Phillips, Peter A. Williams, In *Woodhead Publishing Series in Food Science, Technology and Nutrition, Handbook of Hydrocolloids (Third Edition)*, Woodhead Publishing, 2021, Pages 731-765, ISBN 9780128201046, <https://doi.org/10.1016/B978-0-12-820104-6.00014-0>.
- [52] Menikou G, Damianou C. Acoustic and thermal characterization of agar based phantoms used for evaluating focused ultrasound exposures. *J Ther Ultrasound*. 2017 Jun 1;5:14. doi: 10.1186/s40349-017-0093-z. PMID: 28572977; PMCID: PMC5452295.

- [53] Thu-Hien L. Thanh-Truc N. Van Toi V. *International Journal of Polymer Science*, "Evaluation of the Morphology and Biocompatibility of Natural Silk Fibers/Agar Blend Scaffolds for Tissue Regeneration", Jan. 2018.
- [54] Dabbagh A, Abdullah BJJ, Ramasindarum C, Abu Kasim NH. *Tissue-Mimicking Gel Phantoms for Thermal Therapy Studies. Ultrasonic Imaging*. 2014;36(4):291-316. doi:10.1177/0161734614526372
- [55] Meaney PM, Fox CJ, Geimer SD, Paulsen KD. *Electrical Characterization of Glycerin: Water Mixtures: Implications for Use as a Coupling Medium in Microwave Tomography. IEEE Trans Microw Theory Tech*. 2017 May;65(5):1471-1478. doi: 10.1109/TMTT.2016.2638423. Epub 2017 Jan 31. PMID: 28507391; PMCID: PMC5428894.
- [56] The Engineering Toolbox. "Dielectric Constants of Fluids or Liquids", Apr. 2024.
https://www.engineeringtoolbox.com/liquid-dielectric-constants-d_1263.html
- [57] M.S. Thompson, T.P. Vadala, M.L. Vadala, Y. Lin, J.S. Riffle, Synthesis and applications of heterobifunctional poly(ethylene oxide) oligomers, *Polymer*, Volume 49, Issue 2, 2008, Pages 345-373, ISSN 0032-3861, <https://doi.org/10.1016/j.polymer.2007.10.029>.
- [58] Arvind V. Sarode, Ashok C. Kumbharkhane, Dielectric relaxation study of poly(ethylene glycols) using TDR technique, *Journal of Molecular Liquids*, Volume 164, Issue 3, 2011, Pages 226-232, ISSN 0167-7322, <https://doi.org/10.1016/j.molliq.2011.09.020>.
- [59] D. Bennett, NaCl doping and the conductivity of agar phantoms, *Materials Science and Engineering: C*, Volume 31, Issue 2, 2011, Pages 494-498, ISSN 0928-4931, <https://doi.org/10.1016/j.msec.2010.08.018>.
- [60] *Medical Physics and Biomedical Engineering*. "How to make tissue-equivalent phantoms", Apr. 2024.
<https://www.ucl.ac.uk/medical-physics-biomedical-engineering/research/biomedical-optics-research-laboratory-borl/dot-hub/resources/how-make-tissue-equivalent>
- [61] De Lazzari, M., Ström, A., Farina, L., Silva, N. P., Curto, S., & Trefná, H. D. (2023). Ethylcellulose-stabilized fat-tissue phantom for quality assurance in clinical hyperthermia. *International Journal of Hyperthermia*, 40(1). <https://doi.org/10.1080/02656736.2023.2207797>
- [62] Cheng, K., et al. (2004). "Physical and optical properties of glycerol-water mixtures." *Applied Optics*, 43(28), 5308-5312.
- [63] Ward, A. G., & Courts, A. (1977). *The Science and Technology of Gelatin*. Academic Press.
- [64] Robinson, R. A., & Stokes, R. H. (2002). *Electrolyte Solutions*. Dover Publications.
- [65] Levesque, M. J., & Weng, N. (1980). "Agar-based tissue-equivalent phantom for applications in ultrasound therapy." *Ultrasound in Medicine & Biology*, 6(1), 65-69.
- [66] Brindle, E., et al. (2014). "Role of osmolytes in biophysical properties of tissue phantoms." *Journal of Biomechanics*, 47(8), 1784-1791.

- [67] Rahaman, M. N. (2003). *Ceramic Processing and Sintering* (2nd ed.). CRC Press.
- [68] Niek Exalto, Mario Stassen, Mark Hans Emanuel, Safety aspects and side-effects of ExEm-gel and foam for uterine cavity distension and tubal patency testing, *Reproductive BioMedicine Online*, Volume 29, Issue 5, 2014, Pages 534-540, ISSN 1472-6483
- [69] A. Blazkova, J. Hrivikova, L. Lapcik, "Viscosity properties of aqueous solutions of hydroxyethylcellulose", (1989).
- [70] Kamide, K. (2005). *Cellulose and Cellulose Derivatives: Molecular Characterization and Its Applications*.
- [71] M. H. Seegenschmiedt, P. Fessenden, and C. C. Vernon, *Thermoradiotherapy and Thermochemotherapy: Biology, Physiology, Physics*. Springer, 1995, vol. 1.
- [72] Gabriel, S., Lau, R. W., & Gabriel, C. (1996). The dielectric properties of biological tissues: III. Parametric models for the dielectric spectrum of tissues. *Physics in Medicine & Biology*, 41(11), 2271-2293.
- [73] Bart R. Steensma, Ettore F. Meliadó, Peter Luijten, Dennis W. J. Klomp, Cornelis A. T. Berg, Alexander J. E. Raaijmakers. "SAR and temperature distributions in a database of realistic human models for 7 T cardiac imaging", *NMR In Biomedicine*, 2021.
- [74] Socrates Dokos, "Review of computational methods for therapeutic electromagnetic technologies", *Principles and Technologies for Electromagnetic Energy Based Therapies*, Academic Press, 2022, Pages 25-69, ISBN 9780128205945.

A

Appendix 1

A.1 Dielectric Properties of HEC Gels

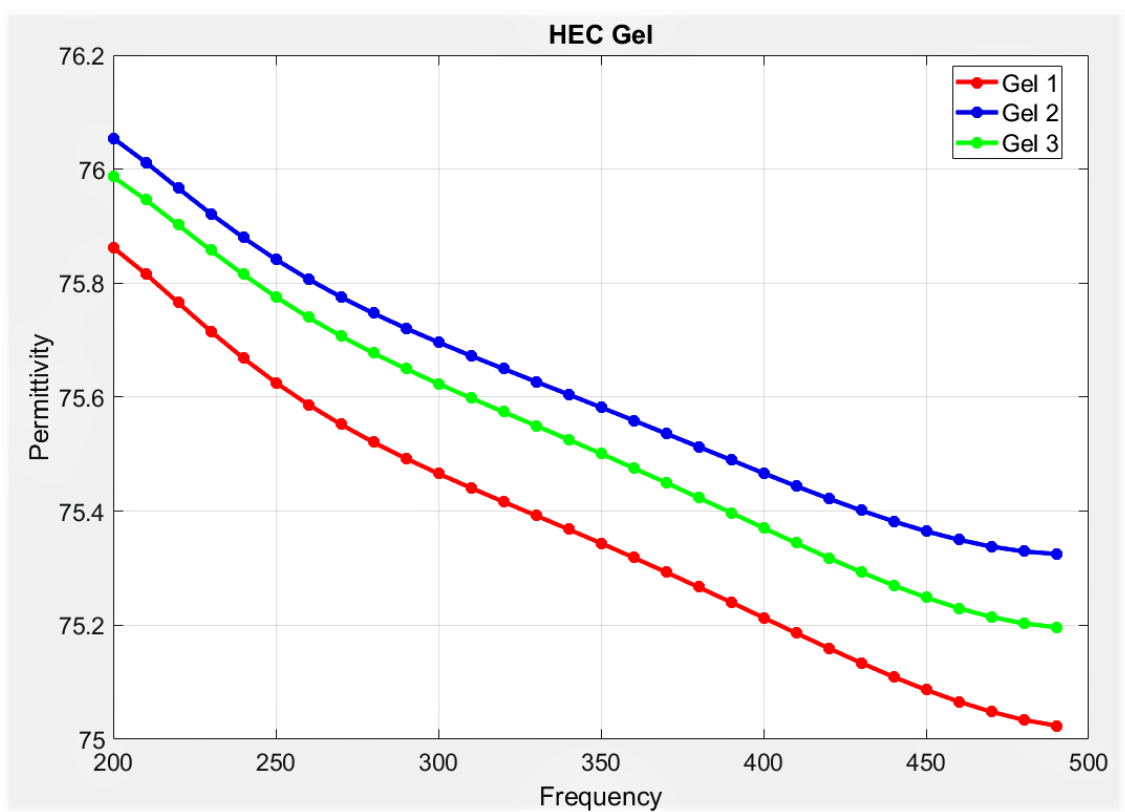


Figure A.1: Permittivity of HEC Gels Over the Frequency Range (200-490 MHz)

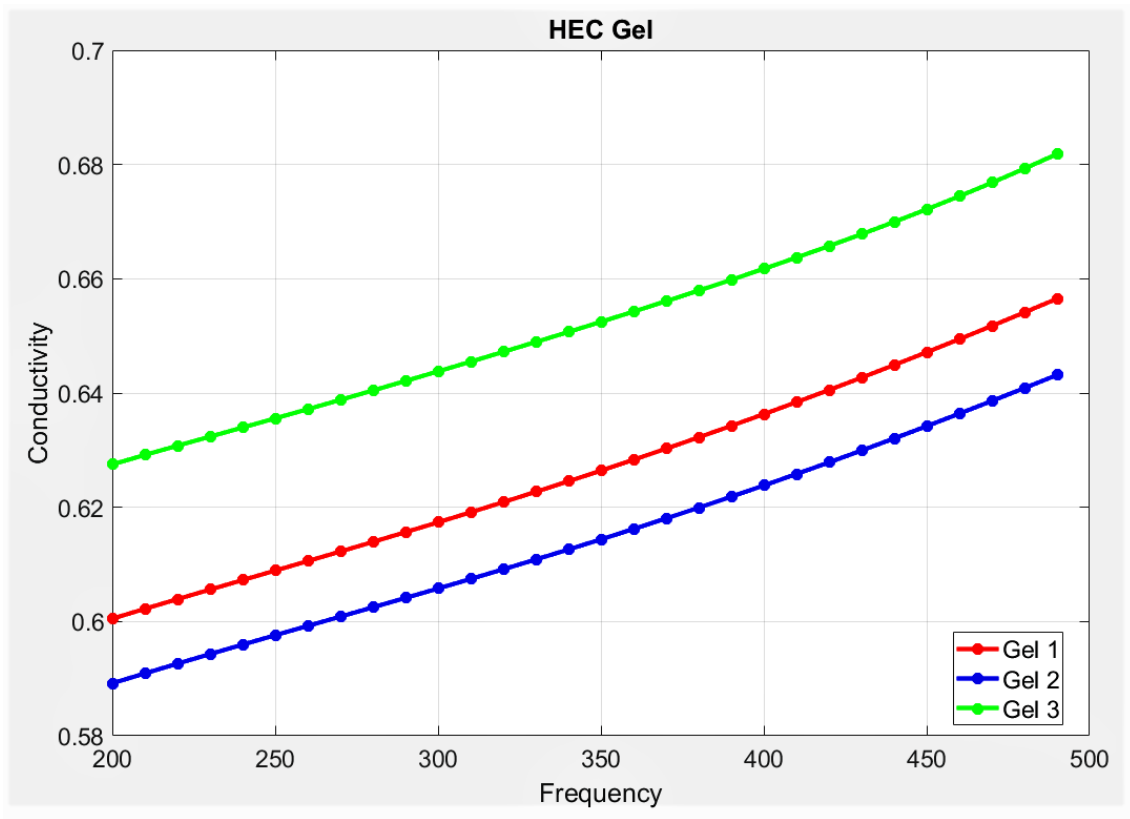


Figure A.2: Conductivity of HEC Gels Over the Frequency Range (200-490 MHz)

DEPARTMENT OF SOME SUBJECT OR TECHNOLOGY
CHALMERS UNIVERSITY OF TECHNOLOGY
Gothenburg, Sweden
www.chalmers.se



CHALMERS
UNIVERSITY OF TECHNOLOGY